

# SAMPLING AND ESTIMATION ON MANIFOLDS USING THE LANGEVIN DIFFUSION

KARTHIK BHARATH\*, ALEXANDER LEWIS†, AKASH SHARMA‡,  
AND MICHAEL V. TRETYAKOV\*

**ABSTRACT.** Error bounds are derived for sampling and estimation using a discretization of an intrinsically defined Langevin diffusion with invariant measure  $d\mu_\phi \propto e^{-\phi} \text{dvol}_g$  on a compact Riemannian manifold. Two estimators of linear functionals of  $\mu_\phi$  based on the discretized Markov process are considered: a time-averaging estimator based on a single trajectory and an ensemble-averaging estimator based on multiple independent trajectories. Imposing no restrictions beyond a nominal level of smoothness on  $\phi$ , first-order error bounds, in discretization step size, on the bias and variances of both estimators are derived. The order of error matches the optimal rate in Euclidean and flat spaces, and leads to a first-order bound on distance between the invariant measure  $\mu_\phi$  and a stationary measure of the discretized Markov process. Generality of the proof techniques, which exploit links between two partial differential equations and the semigroup of operators corresponding to the Langevin diffusion, renders them amenable for the study of a more general class of sampling algorithms related to the Langevin diffusion. Conditions for extending analysis to the case of non-compact manifolds are discussed. Numerical illustrations with distributions, log-concave and otherwise, on the manifolds of positive and negative curvature elucidate on the derived bounds and demonstrate practical utility of the sampling algorithm.

**Keywords:** Ergodic stochastic differential equations, Riemannian manifolds, computing ergodic limits, Monte Carlo technique.

## 1. INTRODUCTION

The Langevin algorithm for sampling from a target probability measure  $d\mu_\phi \propto e^{-\phi(x)} dx$  on  $\mathbb{R}^q$ ,  $q \geq 1$ , is based on constructing a discrete time Markov process  $\{X_n^h, n \geq 1\}$  with time-step size  $h = T/n > 0$ ,  $t_n = hn$ , obtained by discretizing the ergodic Langevin diffusion

$$(1.1) \quad dX(t) = -\frac{1}{2} \nabla \phi(X(t)) dt + dB(t), \quad 0 \leq t \leq T,$$

where  $B(t)$  is the  $q$ -dimensional standard Brownian motion. Popular amongst the numerical methods for constructing  $X_n^h$  is the (explicit) Euler method with Gaussian noise to approximate Brownian motion increments, under which various types of approximation errors in using  $X_n^h$  in place of  $X(t_n)$  have been ascertained [e.g., Roberts and Tweedie, 1996, Dalalyan, 2017, Milstein and Tretyakov, 2007, 2021]. The natural regime to examine error bounds for such algorithms is when step size  $h \rightarrow 0$ .

The Langevin diffusion (1.1) has been successfully used for sampling from posterior distributions in Bayesian inference [e.g., Roberts and Tweedie, 1996, Durmus and Moulines, 2017], for canonical-ensemble calculations in molecular dynamics [Leimkuhler and Matthews, 2015] and

\* SCHOOL OF MATHEMATICAL SCIENCES, UNIVERSITY OF NOTTINGHAM, UK

† INSTITUT FÜR MATHEMATISCHE STOCHASTIK, GEORG-AUGUST-UNIVERSITÄT GÖTTINGEN, GERMANY

‡ DEPARTMENT OF MATHEMATICAL SCIENCES, CHALMERS UNIVERSITY OF TECHNOLOGY AND THE UNIVERSITY OF GOTHENBURG, SWEDEN

for approximating minimizers in convex/non-convex optimisation [e.g., Teh et al., 2016]. Recently, there has been growing interest in finding effective ways to sample from distributions on manifolds, and in providing corresponding theoretical guarantees [e.g., Girolami and Calderhead, 2011, Barp et al., 2022, Gattmirey and Vempala, 2022, Cheng et al., 2022]. Our work aims to provide theoretical guarantees for an intrinsically-defined Langevin algorithm for sampling from a target probability measure on Riemannian manifolds.

In a statistical context, when sampling and estimation are of primary interest, quantitative error bounds, in terms of the time-step  $h$  and integration time  $T$ , on two interconnected quantities related to distributional aspects of the approximations are relevant: bias of an estimator based on  $X_n^h$  of the linear functional  $\mu_\phi(\varphi) := \int \varphi d\mu_\phi$  over a class  $\mathcal{H}$  of test functions  $\varphi$ ; and an integral probability metric with respect to  $\mathcal{H}$  between the stationary measure of  $X_n^h$  and  $\mu_\phi$ . Such bounds are referred to as *weak error bounds*. In statistical applications (e.g., Bayesian computing), the commonly used estimator of  $\mu_\phi(\varphi)$  is based on a single trajectory of  $X_n^h$  until a large time  $N$ , known as the time-averaging estimator. Under suitable conditions on  $\phi$ , when the law of  $X(t)$  converges to its invariant measure  $\mu_\phi$  as  $t \rightarrow \infty$ , it is known that for the Euler method the optimal rate at which bias of the time-averaging estimator disappears is  $O(h)$  [Roberts and Tweedie, 1996, Milstein and Tretyakov, 2007, 2021]; the first-order (in  $h$ ) bound on the bias then results in a commensurate first-order bound on the integral probability metric.

Modern statistical and machine learning applications have generated a growing need for extending the above program to a  $q$ -dimensional smooth Riemannian manifold  $M$ , for example applications in generative AI [Huang et al., 2022, De Bortoli et al., 2022]. To better understand the challenges, some context on the necessary ingredients is helpful. Broadly, nature of the applications engender two perspectives of, and hence coordinate systems on,  $M$ : (i) as a submanifold of  $\mathbb{R}^k, k \geq q$ , with embedded geometry inherited from that of  $\mathbb{R}^k$ ; (ii) as a  $q$ -dimensional differentiable manifold equipped with an intrinsic geometry. These two points of view lead to different formulations of the Langevin diffusion on  $M$  with different invariant measures. The focus of this article is on the intrinsic perspective, and on investigating a geodesic-based sampling algorithm built on an intrinsic Langevin diffusion.

A Riemannian metric  $g$  prescribes a notion of curvature of the manifold  $M$  at a point and determines a unique intrinsic Brownian motion on it [e.g., Elworthy, 1982, Hsu, 2002, Wang, 2013]. The curvature of  $M$  and behavior of the Brownian motion are intimately related: positive curvature makes curves come closer and thus prevents a Brownian motion from wandering away to infinity (non-explosion) while ensuring recurrence and fast convergence to ergodicity [e.g., Ichihara, 1982a,b]; this is true even for its approximation based on a geodesic random walk [Mangoubi and Smith, 2018]. Negative curvature, on the other hand, disperses curves and encourages Brownian motion to exit compact sets and drift away to infinity (explosion) while discouraging recurrence [e.g., Kendall, 1984]. Ricci curvature at a point, which is, roughly, average of the sectional curvatures of two-dimensional subspaces of the tangent space at the point, captures the notion of curvature alluded to above. Compactness (unboundedness) and positive (non-negative) curvature of  $M$  are closely related, although there are non-trivial exceptions depending on the Riemannian metric  $g$  (e.g., manifolds with hyperbolic metric  $g$  [e.g., Everitt and Maclachlan, 2000]). Thus, for negatively curved (typically) non-compact spaces a uniform lower bound on the Ricci curvatures is needed to ensure that the Brownian motion is well-behaved, while this is automatically true for positively curved (typically) compact manifolds. These issues, as one can now imagine, are subtler for a Brownian motion with drift.

It would thus be reasonable to expect the intrinsic curvature of  $M$ , and regularity and decay at infinity of its drift, to influence error of approximations of an intrinsically defined Langevin diffusion and its invariant measure. This is apparently the case in recent works [e.g., Wang et al., 2020, Gutmire and Vempala, 2022, Cheng et al., 2022], where curvature-dependent constant terms show up in upper bounds on distances between the stationary measure  $\mu_\phi^h$  of a discretized Markov processes  $X_n^h$  and  $\mu_\phi$  on  $M$  defined with respect to the Riemannian volume measure  $\text{dvol}_g$ . Importantly, however, the curvature-terms *do not* affect the claimed error order with respect to step size  $h$ .

A differentiable manifold  $M$  is locally Euclidean, covered by a family of charts (open subsets of  $\mathbb{R}^q$ ) and smooth mappings between them. In a small region of  $M$  local analysis of the weak error within a chart, where  $X$  solves the appropriate stochastic differential equation (SDE), proceeds as in  $\mathbb{R}^q$  using the local coordinate representation of the metric  $g$  in the chart, which accounts for the local curvature. The challenge lies in adapting the analysis when one transitions to another chart, where the local representation of the metric  $g$ , and hence that of  $X$ , changes. Thus, on flat manifolds  $M$  with zero curvature, error analysis proceeds unabated as in  $(\mathbb{R}^q, g)$ . Indeed, Mattingly et al. [2010] demonstrate precisely this with weak error analysis when  $M = \mathbb{T}^q \cong \mathbb{R}^q/\mathbb{Z}^q$ , the  $q$ -dimensional compact torus, equipped with the flat (quotient) metric from  $\mathbb{R}^q$ . The main technical ingredient in their analysis was the link between solution of a Poisson equation (given by a partial differential equation (PDE)) on  $\mathbb{T}^q$  and the infinitesimal generator of the Langevin diffusion  $X$ . Aided by the fact that a weak analysis merely requires bounding and matching of a handful of moments, assured by compactness of  $\mathbb{T}^q$ , an *optimal first-order*  $O(h)$  weak error bound, matching the situation in  $\mathbb{R}^q$ , was established for general discretization schemes, including the Euler method.

It thus seems plausible to posit that weak error bounds of a suitable Euler method on compact manifolds  $M$  should match the optimal first-order rate seen on  $\mathbb{T}^q$ . This leads us to the two related questions of interest in this work, stated informally as:

- (Q1) Can an intrinsic Euler discretization method of an intrinsically defined Langevin diffusion on a compact manifold  $M$  match the first-order weak error bounds obtained in the Euclidean setting?
- (Q2) Is it possible to construct estimators of linear functionals of the target measure on  $M$  with first-order bias terms?

**1.1. Contributions and related work.** Our main contribution is in providing affirmative answers to (Q1) and (Q2), and in doing so demonstrate utility of the PDE-based tools in obtaining error bounds of Langevin-based sampling algorithms for compact manifolds. We are unaware of any existing work that achieves this.

Specifically, on a connected compact Riemannian manifold  $(M, g)$  without boundary we consider an intrinsically defined Langevin diffusion

$$dX(t) = -\frac{1}{2}\nabla\phi(X(t))dt + dB^M(t), \quad X(0) = x \in M,$$

with invariant measure  $d\mu_\phi \propto e^{-\phi(x)}d\text{vol}_g$ , where  $B^M$  is a Brownian motion on  $M$ , and its Euler discretization  $X_n^h$  based on moving along geodesics determined by drift-dependent tangent direction and  $\mathbb{R}^q$ -valued noise. The resulting algorithm is termed *Riemannian Langevin*. The potential  $\phi$  is not required to be (geodesically) convex. We emphasize that at every step  $X_n^h$  automatically belongs to the manifold  $M$  thanks to making use of an exponential map (or more generally, retractions), i.e., the algorithm respects the geometry of the problem. It is well-known in deterministic [Hairer et al., 2002] and stochastic [Leimkuhler and Matthews,

2015, Milstein and Tretyakov, 2021] numerical analysis that geometric integrators (i.e., numerical methods which naturally preserve geometric features of differential equations they approximate) are computationally more efficient (e.g., allowing larger time steps while still producing accurate results) for long time simulations as ones arising in sampling problems. The Riemannian Langevin algorithm considered here belongs to the class of such geometric integrators, and is hence suitable for sampling on manifolds.

Two estimators of the linear functional  $\mu_\phi(\varphi)$  for a smooth  $\varphi$  are proposed: an *ensemble-averaging* estimator defined using several independent trajectories of  $X_n^h$ , and a *time-averaging* estimator based on a single trajectory. The former is of great practical merit. First, it enables decoupling and management of three sources of error: (i) length of the integration time  $T$  that controls proximity of  $X$  to its ergodic limit; (ii) discretization error controlled by the step size  $h$ ; (iii) the number of independent trajectories of  $X_n^h$  that controls the Monte Carlo error (sample variance). Second, the estimator is particularly useful in a parallel computing environment (GPUs or array of CPUs) where independent trajectories of  $X_n^h$  can be generated in parallel and combined in the end. Analysis of the time-averaging estimator leads to first-order bound on a distance between the empirical measure  $\mu_\phi^h$  of  $X_n^h$  and  $\mu_\phi$ , with respect to a smooth class  $\mathcal{H}$  of test functions.

Our technical analyses are based on exploiting links between the Markov semigroup of  $X$  and the Kolmogorov and Poisson PDEs; a positive answer to (Q1), bearing in mind the optimal error rate in  $\mathbb{T}^q$ , is realised by effectively ‘flattening’ the compact  $M$ , at least as far as the deviation of the stationary measure  $\mu_\phi^h$  of  $X_n^h$  from  $\mu_\phi$  is concerned. The price paid for the proof technique used is seen in the absence of curvature-related constants in the weak error bounds. However, in addition to deriving the optimal order for weak error, there are other important benefits to the semigroup approach which make it suitable for analyzing sampling algorithms: (i) analysis can be extended to sampling on non-compact manifolds (Section 4); (ii) variants of the Riemannian Langevin algorithm with many families of distributions for increments of the Markov chain  $X_n^h$ , and based on splitting methods, can be analysed in a unified manner (Section 3.2).

The central challenge in extending the analysis to non-compact  $M$  lies in the fact that, unlike when  $M = \mathbb{R}^q$  or a Ricci-flat manifold  $M$  (e.g.,  $\mathbb{T}^q$ ), it is insufficient to merely control the growth of the drift term  $\nabla\phi$ , since the non-positive curvature of  $M$  also dictates behavior of an intrinsic Brownian motion  $B^M$ . The Langevin diffusion can hence fail to be ergodic even when its drift term is well-behaved on a geodesically complete negatively curved  $M$ . We discuss conditions that would enable obtaining first-order weak error bounds in Section 4, and also provide numerical illustrations of the same in Section 5.2, but postpone the theoretical analysis to future work.

As mentioned earlier, there are some existing works that provide curvature-dependent bounds for distances between  $\mu_\phi^h$  and  $\mu_\phi$  under different intrinsic discretizations  $X_n^h$  and settings: Cheng et al. [2022] for the geodesic Euler scheme considered here claim to develop  $O(h^{1/2})$  bound in expected Riemannian distance between  $X(t)$  and  $X_n^h$ ,  $t = nh$ . Gatmiry and Vempala [2022] provide an  $O(h)$  bound on the Kullback-Leibler distance for Hessian manifolds, but assume possibility of *exact* sampling of a Brownian increment on  $M$ , which currently is available only for spheres or products of sphere [Li, 1992]. Further, the above works do not consider and analyse an estimator of  $\mu_\phi(\varphi)$  while we obtain an  $O(h)$  bound on the bias of the estimators.

Although not directly related to our work, we note that there are quite a few papers on extrinsic discretization methods for an embedded Langevin diffusion  $X$  defined by viewing  $M$  as a submanifold of  $\mathbb{R}^k, k \geq q$  [e.g., Lelièvre et al., 2012, Sharma and Zhang, 2021, Laurent and Vilmart, 2022, Armstrong and King, 2022]. A critical limitation of extrinsic methods (with exception of Lie group integrators [e.g., Malham and Wiese, 2008, Davidchack et al., 2009, Mentink et al., 2010, Davidchack et al., 2015] which are only available for SDEs when a Lie group action generates transport along the manifold) is that while  $X$  is constrained to move on  $M$ , the discretized Markov process  $X_n^h$  need not, and repeated projections on to  $M$  are required to ensure that  $X_n^h$  does not leave  $M$ ; this can be computationally expensive. This results in an additional source of error over the original discretization of  $X$ , avoided entirely by intrinsic methods. Intrinsic methods may require additional computation of geodesics when they are unknown in closed-form, but higher-order retractions [e.g., Absil et al., 2008] that are computationally cheaper but do not affect the theoretical weak error bounds are available.

## 2. PRELIMINARIES

In Section 2.1 we briefly review concepts and fix notation from differential geometry needed for analysis on a Riemannian manifold  $M$ ; for more details we refer to some well-known sources [e.g., Jost, 2008, Cheeger and Ebin, 1975, Gallot et al., 1990, Bishop and Crittenden, 2011]. In Section 2.2 we introduce the Langevin diffusion on  $M$  with a given invariant measure, the target measure for sampling.

**2.1. Differential geometric concepts.** Let  $M$  be a  $q$ -dimensional topological manifold. By this we mean a Hausdorff, paracompact, locally Euclidean topological space. We further assume that  $M$  is connected and without a boundary. A chart of  $M$  is a double  $(U, \psi)$  where  $U$  is an open set of  $M$  and  $\psi : M \rightarrow \mathbb{R}^q$  is a homeomorphism. A collection of these charts that cover  $M$  entirely is called an atlas. For any two different charts  $(U_i, \psi_i)$  and  $(U_j, \psi_j)$  that overlap (for any  $i, j$  such that  $U_i \cap U_j \neq \emptyset$ ), the map  $\psi_j \circ \psi_i^{-1} : \psi_i(U_i \cap U_j) \rightarrow \psi_j(U_i \cap U_j)$  is known as a transition map. Then  $M$  is a  $C^k$ -differentiable manifold if the transition maps are  $C^k$  with  $C^k$  inverses. In this paper, we consider the case when  $k = \infty$ , then  $M$  is known as a smooth manifold.

Denote by  $T_x M$  the  $q$ -dimensional tangent space of  $x \in M$  and by  $TM = \cup_x T_x M$  the tangent bundle of  $M$ . A differentiable manifold  $M$  becomes a Riemannian manifold  $(M, g)$  when equipped with a Riemannian metric  $g$ : a family of symmetric bilinear forms that varies smoothly on  $M$ ; dependence on  $g$  is suppressed when the context is clear. The metric  $g$  takes bilinear arguments in the tangent space  $T_x M$  at a point  $x \in M$ .

Denote by  $D$  the unique torsion-free Levi-Civita connection, or covariant derivative, compatible with  $g$ . That is, for  $X, Y, Z \in T_x M$ ,  $D_Z g(X, Y) = g(D_Z X, Y) + g(X, D_Z Y)$  and  $D_X Y - D_Y X - [X, Y] = 0$  for all  $x \in M$ ; here  $[\cdot, \cdot] : T_x M \times T_x M \rightarrow T_x M$  is the Lie bracket on  $TM$  which is defined by  $[X, Y] = XY - YX$  for  $X, Y \in T_x M$ .

The length of a curve  $c : [0, 1] \rightarrow M$  connecting  $c(0) = x$  and  $c(1) = y$  is given by

$$L(c) = \int_0^1 \sqrt{g(\dot{c}(t), \dot{c}(t))} dt,$$

where  $\dot{c} \in T_{c(t)} M$  denotes vector field parallel (the vector field generated) along the curve  $c$ . The curve (or possibly even curves) that minimises the length functional is called a geodesic. A geodesic  $\gamma$  satisfies the equation  $D_{\dot{\gamma}} \dot{\gamma} = 0$ , which in local coordinates takes the form

$$(2.1) \quad \frac{d^2 \gamma^k}{dt^2} + \Gamma_{ij}^k \frac{d\gamma^i}{dt} \frac{d\gamma^j}{dt} = 0,$$

where  $\{\Gamma_{ij}^k\}$  are the Christoffel symbols of  $D$ . The index notation above use the Einstein convention, frequently employed in the paper.

The Riemannian distance  $(x, y) \mapsto \rho(x, y)$  between two points  $x, y \in M$  is defined to be the length of the geodesic  $\gamma$  with  $\gamma(0) = x$  and  $\gamma(1) = y$ . The Riemannian distance is not necessarily injective for given  $x$  and  $y$ . For example, on the  $q$ -dimensional unit sphere  $\mathbb{S}^q$  there are infinitely many geodesics connecting  $x$  and its antipodal point when  $q \geq 2$ . Such a point, where there is more than one geodesic connecting  $x$  to  $y$  is called a cut point of  $x$  (and  $y$ ). The set of such points is called the cut locus of  $x$  and is denoted  $\text{cut}_x$ . The radius of injectivity,  $\text{inj}(x)$  of a point  $x$  on  $M$ , is the radius  $r$  of the largest geodesic ball  $\mathcal{B}_x(r)$  centered at  $x$  such that each geodesic connecting to  $x$  in  $\mathcal{B}_x(r)$  is unique. Then the injectivity radius  $\text{inj}_M$  of the manifold  $M$  is the smallest of such radii across the whole manifold. This leads to the notion of the exponential map.

**Definition 2.1.** For a geodesic  $\gamma : [0, 1] \rightarrow M$  with  $\gamma(0) = x$  let

$$V_x := \{v \in T_x M : \dot{\gamma}(0) = v \text{ and } \gamma(1) \notin \text{cut}_x\}.$$

The mapping  $\exp_x : V_x \rightarrow M$ ,  $v \mapsto \gamma(1)$  is known as the *exponential map* of  $M$  at  $x$ . For  $s \in [0, 1)$ , if  $v$  is such that  $\gamma(s) \in \text{cut}_x$ , we simply define the exponential map as the (non-unique) continuation of  $\gamma$  via  $v$ .

Relatedly,  $M$  is said to be geodesically complete if every geodesic  $\gamma : (-a, a) \rightarrow M$  can be extended to a geodesic with domain  $\mathbb{R}$ , and by the Hopf-Rinow theorem, the space  $(M, \rho)$  is complete as a metric space, and the two notions of completeness coincide. Moreover,  $(M, \rho)$  is said to be compact if it is a compact metric space, and every compact Riemannian manifold without boundary is complete. Note that for a complete  $M$ , continuation of any geodesic  $\gamma$  as in the definition above is thus always possible.

It is necessary to introduce a handful of tensors in preparation for the analysis of the algorithm. First, the exterior derivative  $d$  is a differential operator that maps  $C^1$  functions to the cotangent space  $T_x^* M$ , the dual of the tangent space  $T_x M$ . The local coordinate expression for the exterior derivative is  $df = \frac{\partial f}{\partial x^i} dx^i$ , where  $dx^i$  is a basis in  $T_x^* M$ . The quantity  $df$  is known as a 1-form. More generally, an  $r$ -form, for  $r \in \{1, \dots, q\}$ , can be considered on the  $\wedge^r T_x^* M$  with anti-symmetric wedge product  $\wedge$  spanned by  $dx^1 \wedge \dots \wedge dx^r$ . For brevity, the wedge symbol is omitted when discussing differential forms. Then, the exterior derivative  $d$  maps  $r$ -forms to  $(r+1)$ -forms and  $d^2 = 0$ . For the purposes of integration we introduce the volume form, a  $q$ -form,  $d\text{vol}_g = \sqrt{|g|} dx^1 \dots dx^q$ . Note that  $|g|$  is used for the determinant of the matrix representation of the  $(0, 2)$ -tensor used to represent the Riemannian metric  $g$ .

For  $v \in T_x M$ , the relation

$$df(x)(v) = g(\nabla f(x), v)$$

defines the Riemannian gradient operator  $\nabla$  acting on smooth functions  $f : M \rightarrow \mathbb{R}$  as the dual of  $df$ . In local coordinates, the gradient is written as  $\nabla f = g^{ij} \frac{\partial f}{\partial x^i} \frac{\partial}{\partial x^j}$ ; it is often convenient to omit dependence on  $x$  and use  $df(v)$ ,  $v \in T_x M$ . We also remark that the exterior derivative acting on a function  $df$  is equivalent to the 1-form  $df$ .

The  $L^2$ -adjoint of the gradient is the negative of the divergence operator. For a vector field  $v \in T_x M$ , in local coordinates  $\text{div}(v) = \frac{1}{\sqrt{|g|}} \frac{\partial}{\partial x^i} (\sqrt{|g|} v^i)$ .

The Hessian of a  $C^2$  function  $f : M \rightarrow \mathbb{R}$  is

$$\text{Hess}^f = D^2 f = Ddf.$$

Then, the Laplace–Beltrami operator, as an analogue of the Laplacian from  $\mathbb{R}^q$ , is defined as the trace (with respect to the metric tensor) of the Hessian

$$\Delta f = \text{TrHess}^f = g^{ij} \text{Hess}_{ij}^f.$$

Higher derivatives of  $f$  are obtained by consecutively applying the covariant derivative to  $f$ , e.g. for  $k \geq 0$  derivatives we write this as  $D^k$ .

Define the operator norm for a  $(0, l)$ -tensor  $\mathfrak{T}$  on  $M$

$$(2.2) \quad |\mathfrak{T}|_{\text{op}} := \sup_{V_1, \dots, V_k \in T_x M, |V_i| \neq 0} \frac{|\mathfrak{T}(V_1, \dots, V_k)|}{\prod_{i=1}^k |V_i|}$$

for each  $x \in M$ . In addition to spaces of continuously differentiable functions  $C^l(M)$ , we will need Hölder spaces  $C^{l, \epsilon}(M)$ ,  $0 < \epsilon < 1$ , containing real-valued functions  $u(x)$ ,  $x \in M$ , with corresponding number of Hölder continuous derivatives and with the norm

$$\|u\|_{C^{l, \epsilon}(M)} := \sum_{k=0}^l \sup_{x \in M} |D^k u(x)|_{\text{op}} + \sup_{\gamma_{x,y}, x \neq y \in M} \frac{|D^l u(x) - \Pi_{\gamma_{x,y}}(D^l u(y))|_{\text{op}}}{(\rho(x, y))^\epsilon},$$

where  $\gamma_{x,y}$  denotes any possible minimal geodesic from  $y$  to  $x$  and  $\Pi_{\gamma_{x,y}}$  denotes the parallel transport from  $T_y M$  to  $T_x M$  along  $\gamma_{x,y}$ . Analogously,  $C^{l/2, l, \epsilon}([0, T] \times M)$  is a space of sufficiently smooth functions  $u(t, x)$  with the norm for even  $l$ :

$$\begin{aligned} \|u\|_{C^{l/2, l, \epsilon}([0, T] \times M)} &:= \sum_{k=0}^{l/2} \sum_{n=0}^{l-2k} \sup_{t \in [0, T]} \sup_{x \in M} |D^n \frac{\partial^k}{\partial t^k} u(t, x)|_{\text{op}} \\ &+ \sum_{k=0}^{l/2} \sup_{t \in [0, T]} \sup_{\gamma_{x,y}, x \neq y \in M} \frac{|D^{l-2k} \frac{\partial^k}{\partial t^k} u(t, x) - \Pi_{\gamma_{x,y}}(D^{l-2k} \frac{\partial^k}{\partial t^k} u(t, y))|_{\text{op}}}{(\rho(x, y))^\epsilon}. \end{aligned}$$

For  $X, Y, Z \in T_x M$ , the Riemannian curvature tensor of  $M$  is defined as

$$R(X, Y)Z := (D_X D_Y - D_Y D_X - D_{[X, Y]})Z.$$

When  $X$  and  $Y$  are orthogonal to each other, the final term involving the commutator  $[X, Y]$  vanishes. The sectional curvature at  $x$  is the quadratic form

$$K(X, Y) := g(R(X, Y)Y, X), \quad X, Y \in T_x M,$$

and for an orthonormal basis  $\{X_i\}$  on  $T_x M$ , the Ricci curvature at  $x$  is a contraction of the sectional curvature:

$$\text{Ric}(X, Y) := \sum_{i=1}^d g(R(X, X_i)X_i, Y).$$

**2.2. Langevin diffusion on a Riemannian manifold.** Let  $(M, g)$  be a connected compact Riemannian manifold of dimension  $q \geq 1$  without boundary; this will be main setting assumed throughout the paper except in Sections 4 and 5.2. Consider the target probability measure  $\mu_\phi$  on  $M$

$$(2.3) \quad d\mu_\phi = p \, d\text{vol}_g = \frac{1}{C_\phi} e^{-\phi} d\text{vol}_g,$$

absolutely continuous with density  $p$  with respect to the volume measure  $d\text{vol}_g$ , where  $C_\phi = \int_M e^{-\phi} d\text{vol}_g < \infty$ . The following condition on smoothness of the density  $p$  is imposed through that of  $\phi$ .

*Assumption.* (A1)  $\phi \in C^{3, \epsilon}(M)$ .

No further restrictions are placed on  $\phi$  (e.g., convex). Assumption (A1) ensures that the maps  $x \mapsto g^{ij}(x)$  belong to  $C^{2,\epsilon}(M)$  by the definition of the Hessian as  $D^2\phi$ . The level of smoothness of  $\phi$  in assumption (A1) is required primarily for proofs of Theorems 3.1-3.3, but may be weakened for the content of this section.

Since we aim to sample from a given probability measure  $\mu_\phi$ , we must find an (second order) elliptic linear operator  $\mathcal{A}^*$  acting on probability densities  $p$  (with respect to  $\text{dvol}_g$ ) so that the density  $p$  from (2.3) satisfies the stationary Fokker-Planck equation [Ikeda and Watanabe, 2014, Chapter 5, Proposition 4.5]:

$$(2.4) \quad \mathcal{A}^*p = 0.$$

For example, one can verify that the above is satisfied by the operator

$$(2.5) \quad \mathcal{A}^*p = \frac{1}{2}\Delta_M p + \frac{1}{2}\text{div}(p\nabla\phi),$$

which is adjoint to the elliptic operator [Ikeda and Watanabe, 2014, Chapter 5, Proposition 4.4]

$$(2.6) \quad \mathcal{A} = \frac{1}{2}\Delta_M - \frac{1}{2}g(\nabla\phi, \nabla)$$

acting on  $C^2(M)$ -functions, where  $\Delta_M$  is the Laplace–Beltrami operator.

The Markov process with infinitesimal generator  $\mathcal{A}$  is governed by the following SDE [e.g., Elworthy, 1982, Ikeda and Watanabe, 2014]

$$(2.7) \quad dX(t) = -\frac{1}{2}\nabla\phi(X(t))dt + dB^M(t), \quad 0 \leq t \leq T; \quad X(0) = x,$$

where  $B^M$  is a Brownian motion on the manifold  $M$  defined using the Eells–Elworthy–Malliavin frame bundle construction [e.g., Hsu, 2002, p.87].

The Brownian motion  $B^M$  can be intuited as follows: given a filtered probability space  $(\Omega, \mathcal{F}, \mathcal{F}_t, \mathbb{P}), t \geq 0$ , and an  $\{\mathcal{F}_t\}_{t \geq 0}$ -adapted  $\mathbb{R}^q$ -valued standard Brownian motion  $B$ , the construction uses the dynamics of  $B$  on  $\mathbb{R}^q$  to induce one on  $M$  by pushing forward the dynamics of  $B$  onto the tangent bundle using a (orthonormal) family of frames. Thus, in local coordinates in a chart the SDE (2.7) assumes the Itô's form

$$(2.8) \quad dX^i(t) = -\frac{1}{2}g^{ij}(X_t)\frac{\partial\phi}{\partial x^j}(X(t))dt - \frac{1}{2}g^{kj}(X(t))\Gamma_{kj}^i(X(t))dt + (g^{1/2})^{ij}(X(t))dB_j(t),$$

$$X(0) = x,$$

where  $B_j$  are  $\mathbb{R}$ -valued components of  $B$ . Since  $\phi \in C^{3,\epsilon}(M)$  and, by consequence,  $g^{ij} \in C^{2,\epsilon}(M)$ , (2.8) is well-defined. The frame  $g^{-1/2}(x) : \mathbb{R}^q \rightarrow T_x M$  maps Brownian dynamics from  $\mathbb{R}^q$  to  $T_x M$ , and this leads to the diffusion coefficient  $g^{-1/2}$  in (2.8).

On a Riemannian manifold, not necessarily compact, it is known [Bakry, 1986] that the diffusion  $X$  does not explode, i.e., it is defined for any  $t \geq 0$ , if

$$(2.9) \quad \text{Ric}(v, v) + \text{Hess}(v, v)^\phi \geq -\kappa g(v, v) \quad \text{for all } (x, v) \in TM$$

for some  $\kappa > 0$ . The condition is satisfied for any compact  $M$ , since the Hessian of  $\phi$  is bounded under Assumption (A1); moreover, the Ricci curvature is bounded from below since the sectional curvature at any point in  $M$  is bounded from below [Bishop and Crittenden, 2011, pp. 167]. We will revisit this condition in Section 4 where we discuss the non-compact case.



A key requirement for sampling and estimation using  $X(t)$  is its ergodicity. Recall that a diffusion  $X(t)$  is ergodic if there exists a unique invariant measure  $\mu$  of  $X(t)$ , and independently of the initial condition  $x \in M$ , the limit

$$(2.10) \quad \lim_{t \rightarrow \infty} \mathbb{E}\varphi(X_x(t)) = \int_M \varphi(x) d\mu(x) =: \mu_\phi(\varphi)$$

exists for any bounded function  $\varphi : M \rightarrow \mathbb{R}$ . Furthermore, the process  $X(t)$  is exponentially ergodic if for any  $x \in M$  and any bounded function  $\varphi$  we have the following strengthening of (2.10):

$$(2.11) \quad |\mathbb{E}\varphi(X_x(t)) - \mu_\phi(\varphi)| \leq Ce^{-\lambda t}, \quad t \geq 0,$$

where  $C > 0$  and  $\lambda > 0$  are some constants.

Since the process  $X(t)$  is a non-degenerate diffusion on a compact smooth manifold  $M$ , it converges at an exponential rate to ergodicity [Freidlin, 1985]. By construction, its invariant measure is  $\mu_\phi$ . Consequently, we can exploit the SDE (2.7) (or its local version (2.8)) for computing ergodic limits  $\mu_\phi(\varphi)$ .

Consider two examples of Langevin diffusions on compact  $M$ .

**Example 2.1.** Let  $M = \mathbb{S}^q$  with canonical round metric  $g = dr^2 + \sin^2 r d\theta^2$  with intrinsic coordinate  $x = (r, \theta)$  for  $r \in [0, \pi)$  and  $\theta \in \mathbb{S}^{q-1}$ . The Fisher–Watson distribution has the probability density function  $p(x) \propto \exp(\lambda \cos^2 r)$  with respect to the volume form for  $\lambda > 0$ ,  $r \in [0, \pi)$  [Watson, 1965], and thus  $\phi(x) = -\lambda \cos^2 r$ , which clearly is in  $C^\infty(M) \subset C^{3,\epsilon}(M)$ . Two charts are needed for the local representation of  $X$  since the cut locus of every point is its antipode, and non-empty. The invariant measure exists, and by construction is the Fisher–Watson distribution.

**Example 2.2.** Let  $M = \text{SO}(m)$  be the space of real  $m \times m$  orthogonal matrices with determinant 1, a manifold of dimension  $q = m(m-1)/2$ . Consider the bi-invariant metric  $g(E_1, E_2) = -\frac{1}{2}\text{Tr}(E_1 E_2)$  for  $x \in \text{SO}(m)$ , where  $E_1, E_2 \in T_x \text{SO}(m) \cong \{x\} \times \mathfrak{so}(m)$  and where  $\mathfrak{so}(m)$  is the Lie algebra of  $\text{SO}(m)$  containing skew-symmetric matrices. The matrix generalisation of the von-Mises Fisher distribution, known as the matrix von-Mises distribution [Downs, 1972, Jupp and Mardia, 1979], has the density function  $p(x) \propto \exp(c\text{Tr}(x_0 x))$  for  $c > 0$  and  $x, x_0 \in \text{SO}(m)$ . With  $\phi = -c\text{Tr}(x_0 x)$  it can be verified that for  $x \in \text{SO}(m)$  and  $e \in \mathfrak{so}(m)$ ,  $\text{Hess}^\phi(xe, xe) = -c\text{Tr}(xe^2)$ , which shows that  $\phi \in C^2(M)$  [Lewis, 2023, Section 4.3].

**2.3. Partial differential equations on  $M$  related to the Langevin diffusion.** Central to our analysis of estimators of a linear functional  $\mu_\phi(\varphi)$  of the invariant measure  $\mu_\phi$  are two PDEs that link the generator  $\mathcal{A}$  to  $\mu_\phi(\varphi)$ .

**2.3.1. Backward Kolmogorov PDE.** The backward Kolmogorov PDE on manifold  $M$  associated with the SDE (2.7) [e.g., Ikeda and Watanabe, 2014] is given by:

$$(2.12) \quad \begin{aligned} \frac{\partial u}{\partial t}(t, x) + \mathcal{A}u(t, x) &= 0, & (t, x) \in [0, T] \times M; \\ u(T, x) &= \varphi(x), & x \in M. \end{aligned}$$

Under Assumptions (A1) and  $\varphi \in C^{4,\epsilon}(M)$ , there is a unique solution of the parabolic problem (2.12) which belongs to  $C^{2,4,\epsilon}([0, T] \times M)$  [Aubin, 1998, Ladyzhenskaya et al., 1968, Lunardi, 1995, Ikeda and Watanabe, 2014] and

$$(2.13) \quad \|u\|_{C^{2,4,\epsilon}([0,T] \times M)} \leq C \|\varphi\|_{C^{4,\epsilon}(M)},$$

where  $C > 0$  is a constant independent of a choice of  $\varphi$ .

We need an additional assumption when deriving error bounds of the ensemble-averaging estimator (Theorem 3.1).

*Assumption.* (A2) There exist constants  $\lambda > 0$  and  $C > 0$  that do not depend on  $T$  and choice of  $\varphi$  such that

$$\sum_{k=0}^2 \sum_{n=0}^{4-2k} \left\| \frac{\partial^k}{\partial t^k} u(t, \cdot) \right\|_{C^{n,\epsilon}(M)} \leq C \|\varphi\|_{C^{4,\epsilon}(M)} e^{-\lambda(T-t)}.$$

The above assumption links geometric ergodicity of the Markov process  $X(t)$  solving (2.7) to the decay of the norm of derivatives of its semigroup. In the case of SDEs on  $\mathbb{R}^q$ , the above derivative decay bound was proved under the assumptions of contraction of drift coefficient outside a compact set and uniformly elliptic diffusion coefficient in Talay [1990]. The conditions discussed in Section 2.2 guarantee exponential convergence of the solution to the SDE (2.7) to its invariant measure. The point to be noted here is that under the same conditions the derivative decay bounds are obtained in Talay [1990]. In a bounded subset of  $\mathbb{R}^q$ , a similar result is proved for derivatives of semigroup of reflected diffusion with uniformly elliptic additive noise in Sato et al. [2022]. This is a common assumption in literature dealing with the ensemble-averaging estimation of ergodic limit  $\bar{\varphi}$  (see e.g. Abdulle et al. [2014], Leimkuhler et al. [2023]).

For every  $(t_0, x_0) \in [0, T] \times M$ , the Feynman-Kac formula [Ikeda and Watanabe, 2014, Freidlin, 1985] provides a probabilistic representation of the solution of (2.12) by linking it to the law of the Langevin diffusion  $X(t)$  as

$$(2.14) \quad u(t_0, x_0) = \mathbb{E}(\varphi(X(T))),$$

where  $X$  is from (2.7) with initial condition  $X(t_0) = x_0$ . The representation enables construction of the ensemble-averaging estimator of  $\mu_\phi(\varphi)$  using multiple independent trajectories of the discretized  $X_n^h$ .

**2.3.2. Poisson PDE.** The Poisson PDE on  $M$  associated with the SDE (2.7):

$$(2.15) \quad \mathcal{A}u(x) = \varphi(x) - \mu_\phi(\varphi), \quad x \in M.$$

It is clear that  $\int_M (\varphi(x) - \mu_\phi(\varphi)) d\mu_\phi(x) = 0$ , i.e., the centering condition is satisfied [e.g., Miranda, 1969, Freidlin, 1985]. Under Assumptions (A1) and  $\varphi \in C^{2,\epsilon}(M)$ , there is a unique (upto an additive constant) solution of the elliptic problem (2.15) which belongs to  $C^{4,\epsilon}(M)$  [Aubin, 1998, Nicolaescu, 2007, Miranda, 1969] and

$$(2.16) \quad \|u\|_{C^{4,\epsilon}(M)} \leq C \|\varphi\|_{C^{2,\epsilon}(M)},$$

where  $C > 0$  is a constant independent of a choice of  $\varphi$ .

Using Itô's formula, one can derive the probabilistic representation of solution of (2.15) as [e.g., Freidlin, 1985]

$$u(x) = -\mathbb{E} \int_0^\infty (\varphi(X(t)) - \mu_\phi(\varphi)) dt + \mu_\phi(u).$$

The representation motivates an estimator of  $\mu_\phi(\varphi)$  based on a long single trajectory of  $X_n^h$ , which can then be analysed by the mean ergodic theorem.

### 3. LANGEVIN SAMPLING ALGORITHMS AND ERROR ESTIMATES

Section 3.1 introduces the intrinsic geodesic Euler discretization of the intrinsic Langevin SDE (2.7) to sample from a given distribution  $\mu_\phi$  on a Riemannian manifold. The resulting algorithm can be used on non-compact  $M$  as well, and numerical experiments with the non-compact manifold of symmetric positive definite matrices in Sections 5.2.1 and 5.2.2 demonstrate this. Section 3.2 discusses possible variants and extensions of the Riemannian Langevin algorithm. Section 3.3 provides weak error bounds in the case of compact  $M$ . Section 4 then discusses the sufficient conditions for extension of the weak analysis of the Riemannian Langevin algorithm to non-compact  $M$ .

**3.1. Riemannian Langevin algorithm.** For  $T > 0$  and  $t_0 = 0$ , consider a uniform partition  $t_0 < \dots < t_N = T$  of the interval  $[0, T]$  with time step  $h := T/N$ , i.e.  $t_{n+1} - t_n = h$ ,  $n = 0, \dots, N-1$ . In  $\mathbb{R}^q$ , the Euler method to discretize (1.1) assumes the form (see e.g. Milstein and Tretyakov [2021])

$$X_{n+1}^h = X_n^h - \frac{h}{2} \nabla \phi(X_n^h) + \sqrt{h} \xi_{n+1},$$

where  $\xi_n$ ,  $n = 1, \dots, N$ , are independent standard Gaussians on  $\mathbb{R}^q$  such that  $\sqrt{h} \xi_n$  represents a Brownian increment in a small time step of size  $h$ . Evidently, the dynamics are then along the straight line from  $X_n^h$  with respect to the direction

$$v_{n+1} := -\frac{h}{2} \nabla \phi(X_n^h) + \sqrt{h} \xi_{n+1}.$$

Its natural generalisation to the curved  $M$  is via a Markov process whose next state moves along a geodesic with a direction choosen in the tangent space of the current state. Upon isometrically identifying the tangent space with  $\mathbb{R}^q$ , the following two-step procedure ensues:

- (i) In the tangent space  $T_{X_n^h} M$ , select a random direction  $v_{n+1}$  via an  $\mathbb{R}^q$ -valued random vector  $\xi_{n+1}$ ;
- (ii) follow the geodesic  $[0, 1] \ni t \mapsto \gamma(t) \in M$  with  $\gamma(0) = X_n^h$ ,  $\dot{\gamma}(0) = v_{n+1}$  to  $t = 1$ , and set  $X_{n+1}^h := \gamma(1)$ .

Note that geodesics can be parameterized using the exponential map  $TM \ni (x, v) \mapsto \exp_x(v) \in M$  defined in Section 2.1 such that  $\gamma(1) = \exp_{X_n^h}(v_{n+1})$ , defined using the continuation of  $\gamma$  if  $\gamma(1) \in \text{cut}_{X_n^h}$ .

While the exponential map is injective only in a neighborhood of the origin in a tangent space, geodesic completeness of  $M$  ensures that it is surjective. The two-step procedure is thus well-defined without requiring any restriction on the support of distribution of the random vector  $\xi_{n+1}$ .

However, choice of the distribution of  $\{\xi_n\}$  may be of practical consequence (Section 5.2). Nevertheless, when studying weak convergence, it suffices to consider a distribution that matches  $k$  moments of a Gaussian, where  $k$  is related to the order of weak convergence Milstein and Tretyakov [2021] and in the case of first order weak methods like the Euler scheme it is sufficient to match the first three moments. Thus, in contrast to the algorithms by Cheng et al. [2022] which use Gaussian distributed  $\xi_n$  in  $T_{X_n^h}$  with respect to the inner product  $g(X_n^h)$ , we only require that the components of  $\xi_n^i$ ,  $i = 1, \dots, q$  satisfy

$$(3.1) \quad \mathbb{E}(\xi_n^i) = 0, \quad \mathbb{E}(\xi_n^i)^2 = 1, \quad \mathbb{E}(\xi_n^i)^3 = 0, \quad \mathbb{E}(\xi_n^i)^4 < \infty$$

for every  $n = 0, \dots, N - 1$ . It suffices, for example, to use a discrete distribution so that for each  $n = 0, \dots, N - 1$ ,

$$(3.2) \quad P(\xi_n^i = \pm 1) = \frac{1}{2}, \quad i = 1, \dots, q.$$

The Markov chain  $\{X_n^h, n = 0, 1, \dots, N\}$  with  $X_0^h = x$ , defined as,

$$(3.3) \quad X_{n+1}^h = \exp_{X_n^h} \left( -\frac{h}{2} \nabla \phi(X_n^h) + h^{1/2} g^{-1/2}(X_n^h) \xi_{n+1} \right),$$

represents the discretization of (2.7). The intrinsic method of discretization without using an embedding into  $\mathbb{R}^k$ ,  $k \geq q$ , ensures that it suffices to use a  $q$ -dimensional random vector  $\xi_n$ , as opposed to a higher-dimensional one used in extrinsic approaches [e.g. Laurent and Vilmart, 2022, Sharma and Zhang, 2021, Armstrong and King, 2022].

Importantly, use of the exponential map (or more generally, retractions - see Section 3.2) ensures that  $X_n^h$  always lies on the manifold  $M$ . As discussed in the Introduction, this feature of the algorithms discussed here and in the next subsection is important for their long time stability (in terms of being able to use larger time steps  $h$  and hence resulting in overall faster simulations), which is crucial for efficient sampling.

**3.2. Other Langevin-based sampling algorithms.** Here we consider three variants of the Riemannian Langevin algorithm based on the discrete Markov chain  $X_n^h$  in (3.3), each of which again ensures that  $X_n^h$  always stays on  $M$ .

- Consider different random variables than  $\xi_n$ .

An example is the generalisation of the walk-on-sphere [Milstein and Tretyakov, 2021, Section 7.1.1] on  $\mathbb{R}^q$  to Riemannian manifolds given by

$$(3.4) \quad X_{n+1}^h = \exp_{X_n^h} \left( -\frac{h}{2} \nabla \phi(X_n^h) + \sqrt{q} h g^{-1/2}(X_n^h) \eta_{n+1} \right),$$

where  $\{\eta_n\}$  are independent uniformly, with respect to  $g$ , distributed in the unit sphere  $\{v \in T_{X_n^h} M : g(v, v) = 1\}$  in the tangent space  $T_{X_n^h}$ , and  $\sqrt{q}$  is used to take into account that  $\mathbb{E}(\eta_n^i \eta_n^j) = \delta_{ij}/q$  so that  $\sqrt{q} \eta_n^i$  satisfy the conditions on moments (3.1).

- Consider general maps  $TM \rightarrow M$  in place of the exponential map, which potentially are computationally cheaper when the exponential map is unavailable in closed form.

An example is the Markov chain

$$(3.5) \quad X_{n+1}^h = F_{X_n^h} \left( -\frac{h}{2} \nabla \phi(X_n^h) + h^{1/2} g^{-1/2}(X_n^h) \xi_{n+1} \right),$$

where  $F_x : T_x M \rightarrow M$  is a *retraction*: a smooth map from the tangent bundle  $F : TM \rightarrow M$ , whose restriction  $F_x$  to  $T_x M$  satisfies: (i)  $F_x(0) = x$ ; (ii)  $DF_x(0) = \text{id}_{T_x M}$ , the identity mapping on  $T_x M$ . In the definition, 0 is the origin of the concerned tangent space. See also Remark 3.1.

- Consider splitting methods that divide each iteration of the sampling algorithm into first approximating the drift  $\nabla \phi$  followed by approximating a Brownian increment.

An example is the following Markov chain based on the idea of splitting of the SDE flow [e.g., Milstein and Tretyakov, 2021]:

$$(3.6) \quad \hat{X}_{n+1}^h = F_{X_n^h} \left( -\frac{h}{2} \nabla \phi(X_n^h) \right),$$

$$(3.7) \quad X_{n+1}^h = P_{\hat{X}_{n+1}^h}(h, \xi_{n+1}),$$

where  $F$  can be the exponential map or a retraction as described above,  $\hat{X}_{n+1}^h$  denotes the intermediate step, and  $P(h, \xi_{n+1}) : TM \rightarrow M$  and  $\xi_{n+1}$  are such that

$$(3.8) \quad \mathbb{E}\left(f(P_{\hat{X}_{n+1}^h}(h, \xi_{n+1}))\right) = f(\hat{X}_{n+1}^h) + \frac{h}{2}\Delta_M f(\hat{X}_{n+1}^h) + O(h^2)$$

for any  $f \in C^{4,\epsilon}(M)$ . The above relation can be satisfied, for example, if  $P$  is an exact simulation of Brownian motion from  $t_n$  to  $t_n + h$ , or if

$$(3.9) \quad P_{\hat{X}_{n+1}^h}(h, \xi_{n+1}) = F_{\hat{X}_{n+1}^h}\left(h^{1/2}g^{-1/2}(\hat{X}_{n+1}^h)\xi_{n+1}\right).$$

The sampling method of Gatmiry and Vempala [2022] for Hessian manifolds can be considered as a special case of (3.6)-(3.7) with  $F$  being exponential map at  $X_n^h$  and  $P$  being exact simulation of Brownian motion starting at  $\hat{X}_{n+1}^h$ .

**Remark 3.1.** From proofs of Theorems 3.1-3.3 we note that to achieve bias of order  $O(h)$  for the estimators considered in the sequel, a single step of a standard fourth-order Runge-Kutta scheme for ODEs applied to the geodesic equation at every step of the algorithm (3.3) is sufficient (see Section 5.1 for the use of a Runge-Kutta scheme within the algorithm). In essence, the Runge-Kutta numerical scheme represents a higher-order retraction [Absil et al., 2008, Section 4.1] (see also Remark 5.1).

**3.3. Error bounds.** In this section, first-order weak error bounds are given for the ensemble- and time-averaging estimators of  $\mu_\phi(\varphi) = \int_M \varphi d\mu_\phi$ , based, respectively, on a single and multiple independent trajectories of  $X_n^h$  obtained from (3.3). Proofs of the three theorems stated here are in the Appendix.

**3.3.1. Ensemble-averaging estimator.** Equation (2.11) implies that  $\mu_\phi(\varphi)$  may be estimated upon using  $\mathbb{E}(\varphi(X(T)))$  by choosing a sufficiently large  $T$ . This motivates the ensemble-averaging estimator  $\hat{\mu}_{\phi,N}(\varphi)$  based on independent realizations  $\{X_N^{(m),h}, m = 1, \dots, M\}$  of  $X_n^h$  from the algorithm (3.3) up until the final step  $N$  (recall that  $T = Nh$ ), since

$$(3.10) \quad \hat{\mu}_{\phi,N}(\varphi) = \frac{1}{M} \sum_{m=1}^M \varphi(X_N^{(m),h}) \approx \mathbb{E}(\varphi(X_N^h)) \approx \mathbb{E}(\varphi(X(T))) \approx \mu_\phi(\varphi).$$

A key feature of the estimator is that it allows for a systematic study of three sources of errors influencing its bias: (i) proximity to the ergodic limit controlled by a choice of  $T$ ; (ii) the numerical integration error controlled by the time step  $h$ ; and (iii) the Monte Carlo error controlled by the number of Monte Carlo runs  $M$ . The following result shows how the weak upper bound on its bias depend on both  $h$  and  $T$ , and in a specific way to the class of functions  $\varphi$ .

**Theorem 3.1 (Bias of the ensemble averaging estimator).** *Under Assumptions (A1) and (A2) and  $\varphi \in C^{4,\epsilon}(M)$ , the following bound holds:*

$$(3.11) \quad |\mathbb{E}(\hat{\mu}_{\phi,N}(\varphi)) - \mu_\phi(\varphi)| \leq C(h + e^{-\lambda T}),$$

where  $C, \lambda$  are positive constants independent of  $h$  and  $T$  and the constant  $C$  linearly depends on  $\|\varphi\|_{C^{4,\epsilon}(M)}$  but otherwise  $C, \lambda$  are independent of  $\varphi$ .

Variance of the estimator  $\hat{\mu}_{\phi,N}(\varphi)$  is estimated in the usual way for sample means (see also Section 5):

$$(3.12) \quad \begin{aligned} \text{Var}(\hat{\mu}_{\phi,N}(\varphi)) &= \frac{1}{M} \text{Var}(\varphi(X_N^h)) = \frac{1}{M} [\text{Var}(\varphi(X(T))) + \mathcal{O}(h)] \\ &= \frac{1}{M} [\mu_\phi(\varphi^2) - (\mu_\phi(\varphi))^2 + \mathcal{O}(h + e^{-\lambda T})]. \end{aligned}$$

**3.3.2. Time-averaging estimator.** Since  $X(t)$  is an ergodic process, we also have

$$(3.13) \quad \lim_{T \rightarrow \infty} \frac{1}{T} \int_0^T \varphi(X(t)) dt = \mu_\phi(\varphi), \quad a.s.,$$

which suggests that we can take  $\frac{1}{T} \int_0^T \varphi(X(t)) dt$  as time-averaging estimator for  $\mu_\phi(\varphi)$ . Hence, the numerical time-averaging estimator is

$$(3.14) \quad \tilde{\mu}_{\phi,N}(\varphi) := \frac{1}{N} \sum_{n=0}^{N-1} \varphi(X_n^h).$$

In time-averaging estimation, we simulate a long trajectory and average  $\varphi$  at the discretized points collected along the long trajectory as can be seen in (3.14). There are again three errors associated with the estimator (3.14): (i) due to proximity to the ergodic limit controlled by a choice of  $T$ , (ii) the numerical integration error controlled by the time step  $h$ , and (iii) due to variance of the estimator controlled by  $T$ .

**Theorem 3.2 (Bias and variance of the time-averaging estimator).** *Under Assumption (A1) and  $\varphi \in C^{2,\epsilon}(M)$ , the following bounds hold:*

$$(3.15) \quad |\mathbb{E}(\tilde{\mu}_{\phi,N}(\varphi)) - \mu_\phi(\varphi)| \leq C \left( h + \frac{1}{T} \right),$$

$$(3.16) \quad \mathbb{E}(\tilde{\mu}_{\phi,N}(\varphi) - \mu_\phi(\varphi))^2 \leq C \left( h^2 + \frac{1}{T} \right),$$

where  $C > 0$  is independent of  $h$  and  $T$  and it linearly depends on  $\|\varphi\|_{C^{2,\epsilon}(M)}$  but otherwise it is independent of  $\varphi$ .

**3.3.3. Bound on distance to invariant measure.** The exponential map  $TM \ni (x, v) \mapsto \exp_x(v) \in M$ , and more generally retractions  $F_x$ , are continuous functions of  $x \in M$ . This and Assumption (A1) imply that the recursion

$$X_{n+1}^h = \Phi(X_n^h, \xi_{n+1}).$$

underlying the algorithm engenders a continuous map  $\Phi : M \rightarrow M$  for every realization of  $\xi$ . As a result,  $\{X_n^h\}$  arising from the proposed algorithm is a Feller chain: for a sequence  $x_k \in M$  such that  $\rho(x_k, x) \rightarrow 0$  as  $k \rightarrow \infty$ ,  $\mathbb{E}\varphi(\Phi(x_k, \xi)) \rightarrow \mathbb{E}\varphi(\Phi(x, \xi))$  as  $k \rightarrow \infty$  for  $\varphi$  belonging to the class of bounded and continuous functions. A Feller chain evolving on a compact separable state space has a stationary measure (not necessarily unique) by the Krylov-Bogoliubov theorem [Da Prato and Zabczyk, 1996]. Denote by  $\mu_\phi^h$  a stationary measure of the Markov chain  $X_n^h$  from (3.3). The following result provides an upper bound on an integral probability metric between  $\mu_\phi^h$  and  $\mu_\phi$  with respect to class of test functions.

**Theorem 3.3 (Distance to invariant measure).**

*Under the assumptions of Theorem 3.2, with*

$$\text{dist}(\mu, \nu) := \sup_{\varphi \in \mathcal{H}} \left| \int_M \varphi d\mu - \int_M \varphi d\nu \right|,$$

where  $\mathcal{H} := \{\varphi \in C^{2,\epsilon}(M) \text{ and } \|\varphi\|_{C^{2,\epsilon}(M)} \leq 1\}$ , the following bound holds:

$$(3.17) \quad \text{dist}(\mu_\phi, \mu_\phi^h) \leq Ch,$$

where  $C > 0$  is independent of  $h$ .

**Remark 3.2.** Results similar to those in Theorems 3.1-3.3 can be proved for the three variants of the Riemannian Langevin algorithm discussed in Section 3.2. This is a consequence of our proof techniques, which exploit links between the backward Kolmogorov and Poisson PDEs and the semigroup of the Langevin diffusion.

#### 4. THE CASE OF NON-COMPACT MANIFOLDS

In this section we discuss ingredients needed to transfer the error analysis of the preceding section from compact to non-compact  $M$ . As mentioned in Section 1, negative curvature encourages Brownian motion to drift away to infinity, and a uniform lower bound on the Ricci curvature is needed to address this. Additionally, since non-compactness is closely linked with non-positive curvature, when the Brownian motion has a drift component, as with an  $\mathbb{R}^q$ -valued Brownian motion, extra care is needed.

The condition (2.9) is sufficient to ensure stochastic completeness of a diffusion with generator  $\mathcal{A}$  in (2.6); recall that it is automatically satisfied for compact  $M$ . Hence here we state (2.9) as the below assumption.

*Assumption.* (A3) There exists a  $\kappa > 0$  such that

$$\text{Ric}(v, v) + \text{Hess}^\phi(v, v) \geq -\kappa g(v, v), \quad \text{for all } (x, v) \in TM.$$

We note that this assumption in the case of  $M = \mathbb{R}^q$  resembles a one-sided Lipschitz condition which is sufficient to ensure regularity of SDEs in  $\mathbb{R}^q$  as well as finiteness of moments of their solutions Khasminskii [2012].

Ergodicity, on the other hand, requires more. The *Bakry-Émery criterion* [Bakry and Émery, 1985] demands the existence of a  $\kappa > 0$  such that

$$(4.1) \quad \text{Ric}(v, v) + \text{Hess}^\phi(v, v) \geq 2\kappa g(v, v) \quad \text{for all } (x, v) \in TM,$$

and jointly controls both curvature of  $M$  and drift of the Brownian motion, and is more restrictive than (2.9). For example, when  $M = \mathbb{R}^q$ , the criterion (4.1) reduces to  $\text{Hess}^\phi \geq 2\kappa g$  for  $\kappa > 0$ , and implies that the density  $p$  is  $2\kappa$ -strongly log-concave. The Bakry-Émery criterion provides a sufficient condition for exponential ergodicity of the diffusion (2.7) on non-compact  $M$ , but is redundant for compact  $M$ . Recall that by construction,  $\mu_\phi$  is the invariant measure of the diffusion if it is ergodic.

A few intermediate conditions signpost the route to exponential ergodicity of the Langevin diffusion that satisfies the Bakry-Émery criterion. The criterion ensures that the semigroup  $\{P_t\}$  of operators corresponding to the diffusion satisfy the Log-Sobolev inequality with constant  $2\kappa$  [Wang, 2009], which then implies that they satisfy the Poincaré inequality:  $\text{Var}_{\mu_\phi}(\varphi) \leq C\mathcal{E}(\varphi, \varphi)$  for a Dirichlet form  $\mathcal{E}$  and constant  $C$ . As a consequence, one gets  $|P_t|_{\text{op}} \leq e^{-t/C}$ , which implies exponential ergodicity.

The Bakry-Émery criterion, however, is too stringent for our needs, as it precludes the possibility of sampling from a sizeable class of interesting probability measures on  $M$ . It is instead more natural to impose separate conditions on  $\text{Ric}$  and  $\text{Hess}^\phi$ . The following assumptions are sufficient for the semigroup of operators corresponding to the Langevin diffusion to satisfy the Log-Sobolev inequality [Wang, 2009, Theorem 1.1].

*Assumption.* (A4) For constants  $b, c > 0$ ,  $\text{Ric} \geq (-c - b^2 \rho_o^2)g$ , where  $\rho_o = \rho(o, x)$ ,  $o, x \in M$ .

(A5)  $\text{Hess}^\phi \geq \delta$  outside of a compact set in  $M$ , where the constant  $\delta$  relates to the constants from Assumption (A4) as  $\delta > (1 + \sqrt{2})b\sqrt{q-1} > 0$ .

In the case  $M = \mathbb{R}^q$  Assumption (A5) is  $\delta$ -strong convexity condition to be satisfied outside of a compact set in  $\mathbb{R}^q$  (which means that potential function can be locally non-convex):

$$((x - y), \frac{1}{2}(\nabla\phi(x) - \nabla\phi(y))) \geq \delta|x - y|^2, \quad \delta > 0,$$

which together with constant diffusion coefficient is sufficient for exponential ergodicity of the corresponding SDE in  $\mathbb{R}^q$  [Khasminskii, 2012, Roberts and Tweedie, 1996, Milstein and Tretyakov, 2007].

**4.1. Examples.** A few examples elucidate on Assumptions (A4) and (A5) for non-compact  $M$ .

**Example 4.1.** Let  $M$  be the Poincaré model  $\mathbb{H}^q$  for the  $q$ -dimensional hyperbolic space with metric  $g = \frac{1}{x_q^2} \sum_{i=1}^q dx_i^2$ , under which  $M$  has negative sectional curvature equal to  $-1$  everywhere. From the Cartan–Hadamard theorem, it is diffeomorphic to  $\mathbb{R}^q$ . Consider the Riemannian–Gaussian distribution with density  $p(x) \propto \exp(-\frac{\rho(x,o)^2}{2\sigma^2})$ , with respect to  $\text{dvol}_g$ , where  $o \in M$  is a fixed point and  $\sigma > 0$ ; for brevity, let  $\rho := \rho(x, o)$  be the distance function to the fixed  $o$ .

The Hessian of the squared distance satisfies  $\text{Hess}^{\rho^2} \geq 2g$  [Greene and Wu, 2006], and since  $\mathbb{H}^q$  is an Einstein manifold, its Ricci curvature  $\text{Ric} = -(q-1)g$  has a lower bound. Assumption (A3) is satisfied since  $\text{Ric} + \text{Hess}^\phi \geq (\frac{1}{\sigma^2} - q + 1)g$ , ensuring stochastic completeness. Note that the lower bound need not be positive as  $\sigma > 0$  is unbounded, therefore the Bakry–Émery criterion may be violated for some values of  $\sigma$ .

The lower bound on the Hessian means that we can restrict attention to a geodesic ball centred at  $o$  of finite radius to choose the values  $c = (q-1)$ ,  $b = ((1 + \sqrt{2})\sigma^2\sqrt{q-1})^{-1/2}$  and  $\delta = \frac{1}{\sigma^2}$  such that Assumptions (A4) and (A5) are satisfied in tandem. Convergence exponentially fast to  $p \text{dvol}_g$  is thus assured for any  $\sigma > 0$ , including for values that violate the Bakry–Émery criterion (4.1).

**Example 4.2.** The space  $M = \mathcal{P}_m$  consisting of  $m \times m$  symmetric positive definite matrices with affine-invariant metric  $g$  in (5.6) is a  $q = m(m+1)/2$ -dimensional manifold. As with  $\mathbb{H}^q$ , the space  $\mathcal{P}_m$  with metric  $g$  has a negative sectional curvature everywhere, which, however, unlike  $\mathbb{H}^q$ , is not constant. Assumptions (A3), (A4) and (A5) are verified for the following distributions, later used in Section 5.2.

- (i) Let  $\phi(X) = \frac{1}{2\sigma^2}\rho(X, O)^2$  in (2.3) for  $\sigma > 0$  and fixed  $O \in \mathcal{P}_m$ . This choice of  $\phi$  results in the Riemannian–Gaussian distribution (Section 5.2.1) on  $\mathcal{P}_m$ . It can be verified that  $\text{Ric} \geq -\frac{m}{4}g$ , and by the Hessian comparison theorem  $\text{Hess}^{\rho^2} \geq 2g$  [Lewis, 2023, Section 4.4]. For  $\kappa = |\frac{1}{\sigma^2} - \frac{m}{4}|$ , note that

$$\text{Ric} + \text{Hess}^\phi \geq \left(\frac{1}{\sigma^2} - \frac{m}{4}\right)g,$$

and Assumption (A3) is satisfied. For Assumption (A4), we use the lower bound on the Ricci curvature with  $c = \frac{m}{4}$ . The value of  $b$  can be determined upon first calculating



$\delta$  in Assumption (A5). Since  $\text{Hess}^\phi \geq \frac{1}{\sigma^2}g$ , we select  $\delta = \frac{1}{\sigma^2}$  resulting in an interval  $0 < b < ((1 + \sqrt{2})\sigma^2\sqrt{m-1})^{-1/2}$  of possible values. Hence, Assumptions (A4) and (A5) are satisfied. Note that the Bakry–Émery criterion (4.1) is only satisfied for  $\sigma < \sqrt{\frac{4}{m}}$ .

- (ii) Let  $\phi(X) = \rho(X, O)^4 - \rho(X, O)^2$  in (2.3) for fixed  $O \in \mathcal{P}_m$ . It will be shown in towards the end of this example that  $\phi$  is geodesically non-convex as the Hessian is negative in some domain. To verify Assumption (A3), note that a lower bound on the Ricci curvature is available from (i). To compute the Hessian, consider first a general function  $f \in C^2(\mathcal{P}_m)$ . By the chain rule

$$\text{Hess}^{f(\rho^2)} = f''(\rho^2)d\rho^2 \otimes d\rho^2 + f'(\rho^2)\text{Hess}^{\rho^2}.$$

Then setting  $f(x) = x^2$  results in

$$\text{Hess}^{\rho^4} = 2d\rho^2 \otimes d\rho^2 + 2\rho^2\text{Hess}^{\rho^2},$$

such that Hessian of  $\phi$  is

$$\text{Hess}^\phi = D^2\rho^4 - D^2\rho^2 = 8\rho^2d\rho \otimes d\rho + (2\rho^2 - 1)\text{Hess}^{\rho^2}$$

upon using the fact that  $d\rho^2 = 2\rho d\rho$ . Since  $\text{Hess}^{\rho^2} \geq 2g$  and  $d\rho \otimes d\rho$  is a non-negative tensor:

$$\text{Hess}^\phi \geq 2(2\rho^2 - 1).$$

Thus,  $\text{Ric} + \text{Hess}^\phi \geq (2(2\rho^2 - 1) - \frac{m}{4})g$  and Assumption (A3) is satisfied for  $\kappa = \frac{m+8}{4}$ . Evidently, the Hessian is negative when  $\rho < \frac{1}{\sqrt{2}}$ , hence for the compact set we pick the closure of geodesic ball  $\mathcal{B}_o(1)$  of radius 1 and centred at  $o$ . Outside of this ball, the Hessian is strictly positive, and choosing  $\delta = 2$  ensures that Assumption (A5) is satisfied. This implies that choosing a  $b$  satisfying  $0 < b < (2(1 + \sqrt{2})\sqrt{m-1})^{-1/2}$  takes care of Assumption (A4). Non-convexity of  $\phi$  can now be gleaned from the fact that inside of  $\mathcal{B}_o(1/\sqrt{2})$  the Hessian is negative. To see this, we look at the Hessian contracted with vector fields  $v$  such that  $g(v, \nabla\rho) = 0$ . Then

$$\text{Hess}^\phi(v, v) = (2\rho^2 - 1)\text{Hess}^{\rho^2}(v, v) \leq -2(1 - 2\rho^2)g(v, v) < 0.$$

**4.2. Computational aspects.** When  $M = \mathbb{R}^q$  it is known that Euler-type schemes (including explicit ones) converge when coefficients of the SDE are globally Lipschitz (roughly, when the coefficients grow no faster than linearly at infinity) [Milstein and Tretyakov, 2021]. It is quite straightforward to extend the analysis presented in this paper in the case of compact manifolds to non-compact case under the globally Lipschitz assumption on  $\nabla\phi$  and  $g^{-1/2}$ . This extension will require to prove uniform bounds for moments of  $X_n^h$ .

However, distributions  $\phi$  and manifolds  $(M, g)$  of practical interest are usually so that the globally Lipschitz assumption is violated. It is even so for Example 4.2(i) of the Riemannian–Gaussian distribution on  $\mathcal{P}_m$ .

It is known for SDEs on  $M = \mathbb{R}^q$  that when growth of coefficients at infinity is faster than linear, *explicit* Euler schemes can diverge [Mattingly et al., 2002, Milstein and Tretyakov, 2021, Hutzenthaler et al., 2011]. Reason for the divergence is exploding moments of the corresponding Markov chains (despite moments of the SDEs solution being bounded), typically due to a tiny number of exploding trajectories [Milstein and Tretyakov, 2005, 2021].

By rejecting exploding trajectories, one can safely use any method of weak approximation for a broad class of SDEs with nonglobally Lipschitz coefficients to compute the ensemble

averaging estimator  $\hat{\mu}_{\phi,N}(\varphi)$  of  $\mu_{\phi}(\varphi)$ . SDEs from this class need to merely satisfy stochastic completeness and have sufficiently smooth coefficients, which SDEs of applicable interest typically do. The rejection technique relates to Assumption (A5) in that one can view the condition as ignoring all sample paths of the diffusion that exit a sufficiently large geodesic ball  $\mathcal{B}_o(R)$  for  $R > 0$  around a point  $o \in M$ . Theoretical justification of this when  $M = \mathbb{R}^q$  case is given by Milstein and Tretyakov [2005, 2007] (see also Milstein and Tretyakov [2021]), and it is possible to transfer the proof to the setting of non-compact manifolds  $M$ .

In Section 5.2 we provide numerical evidence of how the rejection technique can profitably be used by choosing a large enough closed geodesic ball, as in Assumption (A5), on  $\mathcal{P}_m$  using the proposed Riemannian Langevin Monte Carlo algorithm. In particular, no trajectory was rejected for  $R = 2.7$  in the case of the Riemannian–Gaussian distribution (Section 5.2.1) and  $R = 2$  for the non-convex potential (Section 5.2.2).

In  $\mathbb{R}^q$ , to address the difficulty with using the explicit Euler scheme for SDEs with nonglobally Lipschitz coefficients in time-averaging estimators, one can use the Metropolis-adjusted Euler scheme [Bou-Rabee and Hairer, 2013]. The Metropolis adjustment also either removes the bias or makes it exponentially small, however it bears substantial additional computational cost. A Metropolis-adjusted version of the Riemannian Langevin algorithm treated in this paper requires a special separate consideration.

Alternatives to the explicit Euler, that result in bounded moments, have been studied in depth for SDEs in  $\mathbb{R}^q$  with non-globally Lipschitz coefficients. Examples include implicit methods (and in particular, the implicit Euler scheme) and explicit methods of tamed and balanced type [e.g., Mattingly et al., 2002, Hutzenthaler and Jentzen, 2015, Tretyakov and Zhang, 2013, Milstein and Tretyakov, 2021]. Extensions of such methods to the non-compact manifold setting are possible and will be taken up elsewhere.

## 5. NUMERICAL ILLUSTRATIONS

We carry out numerical experiments to verify the theoretical results from Section 3.3 for compact manifolds  $M$ , and demonstrate utility of the proposed algorithm for both compact and non-compact  $M$ . Section 5.1 considers sampling from the von-Mises distribution on the two-dimensional unit sphere  $\mathbb{S}^2$ ; sampling algorithms using extrinsic embedding coordinates was proposed by Wood [1994], and a method using intrinsic coordinates was proposed by Best and Fisher [1979]. Both algorithms use rejection sampling, with the latter method appropriate only for very small or large concentrations.

Section 5.2 considers two distributions on the non-compact manifold of symmetric positive definite matrices: the Riemannian–Gaussian distribution with convex  $\phi$ , and a distribution with non-convex potential. Versatility of the proposed algorithm to handle both convex and non-convex potential is demonstrated.

We focus on the ensemble-averaging estimator  $\hat{\mu}_{\phi,N}(\varphi)$  in (3.10), simulate a large number  $M$  of trajectories for a sufficiently long time  $N$ , and then verify that it enjoys first order of convergence in terms of time step  $h$  by comparing with the exact value of  $\mu_{\phi}(\varphi)$  (obtained via numerical integration). Two types of errors are reported: the estimation error

$$\mathbf{err} = |\hat{\mu}_{\phi,N}(\varphi) - \mu_{\phi}(\varphi)|;$$

and, the Monte Carlo error

$$\mathbf{MCerr} = \frac{1}{M-1} \left( \sum_{m=1}^M \varphi(X_N^{(m),h})^2 - \frac{1}{M} \left( \sum_{m=1}^M \varphi(X_N^{(m),h}) \right)^2 \right),$$

with corresponding 95% confidence interval

$$\hat{\mu}_{\phi,N}(\varphi) \pm 1.96 \sqrt{\frac{\text{MCerr}}{M}}.$$

We note that in a similar manner, the theoretical results (see Theorem 3.2) for the time-averaging estimator  $\hat{\varphi}_N$  (3.14) can also be verified.

Simulations were performed in **R** using a parallel architecture on 30 cores, using the packages **purrr** and **furrr** on a Supermicro 620U Linux RHEL8.8 server with 48 Intel Xeon (Ice Lake class) CPUs.

**5.1. Unit sphere with the von-Mises Fisher distribution.** The unit sphere  $\mathbb{S}^2$  is a compact manifold with constant positive sectional curvature 1 everywhere, such that the cut locus of every point  $x$  is its antipode  $-x$ . This means that a single chart cannot cover  $\mathbb{S}^2$  in order to implement the proposed algorithm. Charts can be defined by embedding  $\mathbb{S}^2$  into  $\mathbb{R}^3$ , and this is commonly done using the inclusion map as the embedding such that  $\mathbb{S}^2 = \{(x_1, x_2, x_3)^\top \in \mathbb{R}^3 : x_1^2 + x_2^2 + x_3^2 = 1\}$ , and two stereographic projections from the north and south poles onto  $\mathbb{R}^2$  are used to define two charts which cover  $\mathbb{S}^2$ .

We will instead consider spherical coordinates arising from the embedding of  $\mathbb{S}^2$  into  $\mathbb{R}^2$  given by  $(r, \theta)^\top \mapsto (\sin r \cos \theta, \sin r \sin \theta, \cos r)^\top$ , where  $r$  is the geodesic distance to the north pole, with  $r \in [0, \pi]$ ,  $\theta \in [0, 2\pi]$ . Our choice is motivated by the fact that expressions for the exponential and inverse-exponential maps are not available analytically in spherical coordinates, and implementation of the proposed algorithm thus requires approximating the exponential map by numerically solving the geodesic equation. As mentioned in Remark 3.1, a good approximation of the exponential map preserves the order of errors derived in Section 3.3, and we verify this numerically (see also Remark 5.1 below).

The Riemannian metric for the spherical coordinates at a point  $x = (r, \theta)^\top$  is

$$(5.1) \quad g = dr^2 + \sin^2 r d\theta^2,$$

which is obtained by the pulling back the Euclidean metric from  $\mathbb{R}^3$ . The inverse metric tensor assumes the form

$$G^{-1} = \begin{pmatrix} 1 & 0 \\ 0 & \frac{1}{\sin^2 r} \end{pmatrix},$$

which is unbounded at  $r = 0$  or  $r = \pi$  or equivalently, at  $(0, 0, 1)^\top$  or  $(0, 0, -1)^\top$  in  $\mathbb{R}^3$ , and can lead to instability or loss of accuracy of the algorithm. The second chart is acquired by an orthogonal transformation of the coordinate axes obtained by permuting the axes corresponding to the embedding  $(r, \theta)^\top \mapsto (\cos r, \sin r \cos \theta, \sin r \sin \theta)^\top$  with the metric unchanged. The transition map between the charts is then

$$(5.2) \quad \psi(r, \theta) = (\arccos(\sin r \cos \theta), \arctan(\cot r \csc \theta))^\top,$$

which in  $\mathbb{R}^3$  maps  $(\sin r \cos \theta, \sin r \sin \theta, \cos r)^\top \mapsto (\cos r, \sin r \cos \theta, \sin r \sin \theta)^\top$ ; its inverse is

$$(5.3) \quad \psi^{-1}(\tilde{r}, \tilde{\theta}) = (\arccos(\sin \tilde{r} \sin \tilde{\theta}), \arctan(\tan \tilde{r} \cos \tilde{\theta}))^\top.$$

Numerically, we restrict the domain of the embeddings to  $(\epsilon, \pi - \epsilon) \times [0, 2\pi]$  for some  $\epsilon > 0$ , whence the union of the two charts covers  $\mathbb{S}^2$  as the singular points  $r = 0$  and  $r = \pi$  in chart 1 are mapped to  $(\pi/2, \pi/2)$  and  $(\pi/2, 3\pi/2)$ , respectively, for any  $\theta \in [0, 2\pi]$ . We choose  $\epsilon = 0.5$  in the simulations, which ensures that  $G^{-1}$  is bounded.

The centred von-Mises Fisher distribution  $\mu_\phi$  on  $\mathbb{S}^2$  is the distribution

$$(5.4) \quad d\mu_\phi \propto e^{\lambda \cos r} d\text{vol}_g, \quad \text{for } \lambda > 0, r \in [0, \pi],$$

so that  $\phi((r, \theta)^\top) = \lambda \cos r$ ; performance of the algorithm for a non-centred version can be examined with obvious modifications. It was verified in Example 2.1 that the Langevin diffusion (2.7) with  $\phi((r, \theta)^\top) = -\lambda \cos r$  is ergodic, and converges exponentially fast to its invariant measure  $\mu_\phi$ .

The geodesic equation (2.1) can be written as the following system of ODEs in local coordinates starting at  $(r_0, \theta_0)^\top$ :

$$(5.5) \quad \begin{aligned} \dot{r} &= y, \quad r(0) = r_0, \\ \dot{\theta} &= z, \quad \theta(0) = \theta_0, \\ \dot{y} &= \sin r \cos r \, z^2, \quad y(0) = v^1, \\ \dot{z} &= -2 \cot r \, yz, \quad z(0) = v^2. \end{aligned}$$

The ODEs are solved using a single step of size  $\sqrt{h}$  of the standard  $(1/6, 1/3, 1/3, 1/6)$  4th-order Runge–Kutta method (RK4) [Hairer et al., 1993]. It approximates the solution to the geodesic equation in local coordinates within each chart and hence stays on the manifold for all time. Since the one-step accuracy of RK4 method is of fifth order, the error of our approximation of the geodesic equation at each step of the algorithm is of order  $O(h^{5/2})$  which is smaller than the one-step error  $O(h^2)$  of the Euler method (see Lemma A.1); the additional error incurred from having to approximate the exponential map hence does not affect the convergence order  $O(h)$  of the algorithm.

---

**Algorithm 5.1** Sample from a von-Mises Fisher distribution on  $\mathbb{S}^2$ .

---

- (1) Input  $\lambda, h, N, X_0$
  - (2) Initialise the chain at  $X_0 = (r_0, \theta_0)^\top$  according to the first chart and set chart counter  $c = 1, \epsilon = 0.5$  and  $n = 0$ .
  - (3) If  $r_n < \epsilon$  or  $r_n > \pi - \epsilon$ :  
     if  $c = 1$ , change the chart according to (5.2) and set  $c = 2$ ;  
     if  $c = 2$ , change the chart according to (5.3) and set  $c = 1$ .
  - (4) Generate  $\xi_{n+1} = (\xi_{n+1}^1, \xi_{n+1}^2)^\top$ , where  $\xi_{n+1}^i$  are independent, from (3.2).
  - (5) Construct the vector field:  
     if  $c = 1$ , set  $v_{n+1} = -\frac{\lambda\sqrt{h}}{2} \sin r_n (1, 0)^\top + g^{-1/2}(X_n^h) \xi_{n+1}$ ;  
     if  $c = 2$ , set  $v_{n+1} = \frac{\lambda\sqrt{h}}{2} (\cos r_n \sin \theta_n, \csc r_n \cos \theta_n)^\top + g^{-1/2}(X_n^h) \xi_{n+1}$ .
  - (6) Approximate the geodesic equation (5.5) with  $(r_0, \theta_0)^\top = (r_n, \theta_n)^\top, (v^1, v^2)^\top = (v_{n+1}^1, v_{n+1}^2)^\top$  by a single step of size  $\sqrt{h}$  of RK4 to obtain  $X_{n+1}^h = (r_{n+1}, \theta_{n+1})^\top$ .
  - (7) **If**  $n + 1 = N$  then **stop** and if  $c = 2$ , change  $X_N^h$  to first chart according to (5.2), **else** put  $n := n + 1$  and **return** to Step 3.
- 

We used  $\varphi(x) = \sin r$ , and compute, for  $\lambda = 1$ , the exact value  $\mu_\phi(\varphi) = \sqrt{2} \frac{I_1(1)\Gamma(3/2)}{I_{1/2}(1)}$ , where  $I_n(\lambda)$  is the modified Bessel function of the first kind [Lewis, 2023, Section 4.1]. The algorithm was terminated at time  $T = 5$ , sufficient to ensure that the error  $|\mathbb{E}(\varphi(X(T))) - \mu_\phi(\varphi)|$  (i.e., the error due to proximity of the SDE’s solution to the ergodic limit) is negligibly small. From Table 1 and the black line in Figure 1, we observe the first order convergence of Algorithm 5.1 as expected.

We also report results from an experiment with the modified Algorithm 5.1 in which the discrete random variables  $\xi$  distributed according to (3.2) are replaced with standard Gaussian random variables. The corresponding results given in Table 2 and the blue line in Figure 1 show first order convergence of Algorithm 5.1 with Gaussian random variables. Interestingly,

$h$	$M$	err	MCerr
0.2	$10^6$	0.0239	0.0004
0.1	$10^6$	0.0068	0.0004
0.05	$10^6$	0.0029	0.0005
0.025	$10^7$	0.0014	0.0001
0.0125	$10^7$	0.00065	0.00015
0.01	$10^7$	0.00048	0.00015

TABLE 1. Estimation and Monte Carlo errors for sampling from a von-Mises Fisher distribution. The parameters are  $\lambda = 1$ ,  $X_0 = (r_0, \theta_0)^\top = (\pi/4, \pi/4)^\top$  and  $T = 5$ .

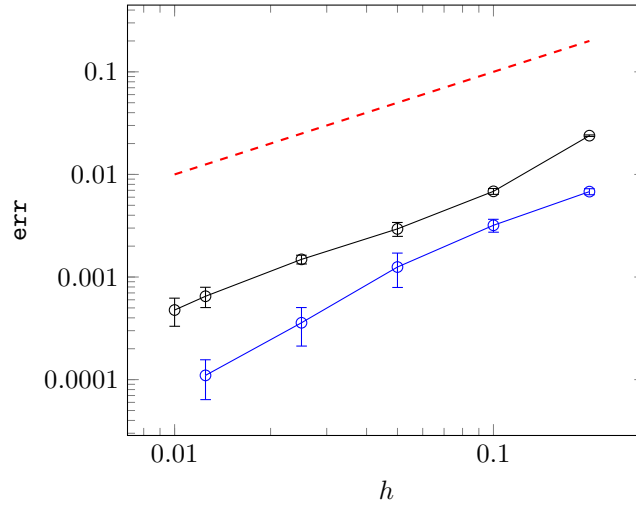


FIGURE 1. Sampling from a von-Mises Fisher distribution. A log-log plot of the error **err** against  $h$ . The black (blue) line corresponds to the Algorithm 5.1 with  $\xi_n$  distributed according to (3.1) (standard Gaussian distribution). Error bars correspond to Monte Carlo error **MCerr**. The reference red line has gradient 1. The parameters are as in Table 1.

$h$	$M$	err	MCerr
0.2	$10^6$	0.0068	0.0005
0.1	$10^6$	0.0032	0.0005
0.05	$10^6$	0.0013	0.0005
0.025	$10^7$	0.00036	0.00015
0.0125	$10^8$	0.00011	0.00005

TABLE 2. Sampling from a von-Mises Fisher distribution (Algorithm 5.1 with Gaussian  $\xi$ ). The parameters are as in Table 1.

the error is smaller in the case of Gaussian random variables than when the discrete random variables are used.

**Remark 5.1.** RK4 method can be viewed as a high order retraction since by solving numerically the geodesic equation we are approximating the exponential map. Specifically, the method is a mapping from  $T\mathbb{S}^2$  to  $\mathbb{S}^2$  with local truncation error of order  $O(h^{5/2})$  at time  $h^{1/2}$ . See [Absil et al., 2008, Section 4.1] for further details on retractions.

**5.2. Symmetric positive definite matrices.** We consider the non-compact manifold of symmetric positive definite matrices, and demonstrate numerically that the proposed algorithm results in the desired error bounds when sampling from two distributions which satisfy the assumptions discussed in Section 4.

Consider the general linear group  $GL(m)$  consisting of the set of  $m \times m$  real invertible matrices equipped with the group operation of matrix multiplication. Denote by  $M = \mathcal{P}_m$ , the manifold of  $m \times m$  symmetric positive definite matrices  $\mathcal{P}_m = \{X \in GL(m) : X^\top = X, y^\top X y > 0, y \in \mathbb{R}^m\}$ , an open cone of dimension  $q = m(m+1)/2$ .

The tangent space  $T_X \mathcal{P}_m = \{X\} \times \mathcal{S}_m$ , where  $\mathcal{S}_m$  is the set of  $m \times m$  real symmetric matrices. Various choices of metric are available on  $\mathcal{P}_m$  [Pennec et al., 2006], and we choose the affine invariant metric

$$(5.6) \quad g(U, V)_X = \text{Tr}(X^{-1} U X^{-1} V), \quad U, V \in T_X \mathcal{P}_m,$$

which is invariant under the transformation  $X \mapsto A^{-1} X A$ , for every  $A \in GL(m)$ . The metric is compatible with the transitive action of  $GL(m)$  on  $\mathcal{P}_m$  in that between any pair  $X_1, X_2 \in \mathcal{P}_m$  there exists an  $A \in GL(m)$  such that  $X_2 = A^{-1} X_1 A$ , which makes  $\mathcal{P}_m$  a homogeneous space of  $GL(m)$ .

Affine invariance of the metric ensures that the Riemannian distance  $\rho$  and volume form  $\text{dvol}_g$  will also be invariant under affine transformations. The metric  $g$  gives  $\mathcal{P}_m$  a Riemannian structure with non-positive sectional curvature, and  $\mathcal{P}_m$  is a non-compact, geodesically complete metric space by the Hopf–Rinow theorem [e.g., Jost, 2008]. Moreover, by the Cartan–Hadamard theorem [e.g., Kobayashi and Nomizu, 1969], the inverse exponential map is globally defined, and the cut locus of every point is empty, i.e., every two points in  $\mathcal{P}_m$  have a unique geodesic connecting them. This means that only a single chart is needed to cover  $\mathcal{P}_m$ .

The volume form at a point  $X \in \mathcal{P}_m$  with affine-invariant metric  $g$  is

$$\text{dvol}_g = \det(X)^{(m+1)/2} dx_1 \dots dx_{m(m+1)/2},$$

where  $x_1, \dots, x_{m(m+1)/2}$  are the upper triangular elements of  $X$ . For  $X \in \mathcal{P}_m$  and  $S \in \mathcal{S}_m$ , the exponential map has the closed form

$$(5.7) \quad \exp_X(tS) = X^{1/2} \text{Exp}(tX^{-1/2} S X^{-1/2}) X^{1/2},$$

where  $\text{Exp}$  is the matrix exponential. A geodesic that connects two points  $X_1, X_2 \in \mathcal{P}_m$  can be parameterised as

$$\gamma(t) = X_1^{1/2} \text{Exp}(t \text{Log}(X_1^{-1/2} X_2 X_1^{-1/2})) X_1^{1/2}$$

so that  $\gamma(0) = X_1$  and  $\gamma(1) = X_2$ , where  $\text{Log}$  is the matrix logarithm defined globally on  $\mathcal{P}_m$ . The distance between two points  $X_1$  and  $X_2$  is

$$\rho(X_1, X_2) = \sqrt{\sum_{i=1}^n (\log r_i)^2},$$

where  $\{r_i\}_{i=1}^m$  are the eigenvalues of  $X_1^{-1}X_2$ . The inverse exponential map can also be written in the closed form:

$$(5.8) \quad \exp_{X_1}^{-1}(X_2) = \dot{\gamma}(0) = X_1^{1/2} \text{Log}(X_1^{-1/2} X_2 X_1^{-1/2}) X_1^{1/2}.$$

For efficient use of the coordinates, we consider the vectorization and half-vectorization maps. With  $\text{vec} : \mathcal{S}_m \rightarrow \mathbb{R}^{m^2}$  as the vectorization map taking a symmetric matrix to a column vector, consider the half-vectorization map

$$\text{hvec} : \mathcal{S}_m \rightarrow \mathbb{R}^q, \quad \text{hvec}(x) := B \text{vec}(x),$$

where the matrix

$$B := \sum_{i \geq j} (u_{ij} \otimes e_j^\top \otimes e_i^\top) \in \mathbb{R}^{q \times m^2}$$

picks out the lower triangular part of the vectorization, and  $u_{ij}$  is a  $q$ -dimensional unit vector with 1 in position  $(j-1)m + i - j(j-1)/2$  and 0 elsewhere, and  $e_i$  is the standard basis of  $\mathbb{R}^{m^2}$ . Its inverse

$$\mathbb{R}^q \ni x \mapsto \text{hvec}^{-1}(x) := (\text{hvec}(I_m)^\top \otimes I_m)(I_m \otimes x) \in \mathbb{R}^{m \times m}$$

exists through the Moore-Penrose inverse of  $A$ .

For the experiments, we fix  $m = 3$  and consider  $\mathcal{P}_3$  with global coordinates  $x = (x_1, x_2, x_3, x_4, x_5, x_6)$  such that

$$X = \begin{pmatrix} x_1 & x_4 & x_6 \\ x_4 & x_2 & x_5 \\ x_6 & x_5 & x_3 \end{pmatrix}.$$

The metric tensor  $G$  is expressed as  $G = dx^\top (X^{-1} \otimes X^{-1}) dx$ , where  $dx := \text{hvec}(dX)$  with  $dX = (dx_i)$ . The inverse metric  $G^{-1}$  can be concisely expressed [e.g., Moakher and Zéraï, 2011]:

$$G^{-1}(X) = \begin{pmatrix} x_1^2 & x_4^2 & x_6^2 & x_1 x_4 & x_4 x_6 & x_1 x_6 \\ x_4^2 & x_2^2 & x_5^2 & x_2 x_4 & x_2 x_5 & x_4 x_5 \\ x_6^2 & x_5^2 & x_3^2 & x_5 x_6 & x_3 x_5 & x_3 x_6 \\ x_1 x_4 & x_2 x_4 & x_5 x_6 & \frac{1}{2}(x_1 x_2 + x_4^2) & \frac{1}{2}(x_2 x_6 + x_4 x_5) & \frac{1}{2}(x_1 x_5 + x_4 x_6) \\ x_4 x_6 & x_2 x_5 & x_3 x_5 & \frac{1}{2}(x_2 x_6 + x_4 x_5) & \frac{1}{2}(x_2 x_3 + x_5^2) & \frac{1}{2}(x_3 x_4 + x_5 x_6) \\ x_1 x_6 & x_4 x_5 & x_3 x_6 & \frac{1}{2}(x_1 x_5 + x_4 x_6) & \frac{1}{2}(x_3 x_4 + x_5 x_6) & \frac{1}{2}(x_1 x_3 + x_6^2) \end{pmatrix},$$

which must be written as a column vector in  $\mathbb{R}^6$  using the  $\text{hvec}^{-1}$  map for use in the algorithms.

**5.2.1. Riemannian–Gaussian distribution.** The Riemannian–Gaussian distribution can be viewed as the generalisation of the isotropic normal distribution on  $\mathbb{R}^q$  to  $\mathcal{P}_m$ , where the Euclidean distance is replaced by the Riemannian distance in the probability density function:

$$d\mu_\phi(X) = \frac{1}{Z_m(\sigma)} e^{-\phi(X)} d\text{vol}_g, \quad X \in \mathcal{P}_m,$$

where

$$(5.9) \quad \phi(X) = \frac{1}{2\sigma^2} \rho(X, O)^2$$

for a fixed  $O \in \mathcal{P}_m$  and parameter  $\sigma > 0$ . The function  $x \mapsto \phi(x)$  is strictly convex, since, by the Hessian comparison theorem [Cheeger and Ebin, 1975] the map  $x \mapsto \rho(x, \cdot)^2$  is geodesically convex on a manifold with everywhere non-positive sectional curvature. The Riemannian–Gaussian distribution is hence log-concave.

The normalisation constant  $Z_m(\sigma)$  can be evaluated by employing spectral decomposition  $X = Q^\top \text{diag}(e^{\lambda_1}, \dots, e^{\lambda_m}) Q$ , with eigenvalues  $\lambda_1 \geq \dots \geq \lambda_m > 0$ , and computing the following integral

$$(5.10) \quad c_m \int_{\mathbb{R}^m} e^{-\frac{1}{2\sigma^2}[\lambda_1^2 + \dots + \lambda_m^2]} \prod_{i < j} \sinh\left(\frac{|\lambda_i - \lambda_j|}{2}\right) d\lambda_1 \dots d\lambda_m,$$

where  $c_m = \frac{1}{m!} \frac{\pi^{m^2/2}}{\Gamma_m(m/2)} 8^{m(m-1)/4}$  and  $\Gamma_m$  is the multivariate gamma function [Said et al., 2017]; the constant  $c_m$  is part of the volume form  $\text{dvol}_g$ , and when  $m = 3$ ,  $c_3 = \frac{16\sqrt{2}\pi^2}{3}$ . Without loss of generality we set  $O = I_m$ , since  $\mathcal{P}_m$  is a homogeneous space. For convenience, we use  $\rho_I = \rho_I(X) := \rho(X, I_m)$ .

$h$	$M$	err	MCerr
0.2	$10^6$	0.148	0.008
0.1	$10^6$	0.078	0.008
0.05	$10^7$	0.035	0.002
0.025	$10^7$	0.017	0.002

TABLE 3. Estimation and Monte Carlo errors for the Riemannian—Gaussian distribution. The parameters are  $O = I_3$ ,  $\sigma = \frac{1}{\sqrt{2}}$ ,  $X_0 = \text{hvec}^{-1}((2, 4, 2, 1, 1, 0)^\top)$  and  $T = 10$ .

To our knowledge, currently, only a rejection-based algorithm for sampling from Riemannian–Gaussian on  $\mathcal{P}_m$ , which relies on sampling the eigenvalues, is available in the literature [Said et al., 2017]. Our Riemannian Langevin algorithm given in Algorithm 5.2 does not contain a rejection step; however, a rejection step can in principle be incorporated if needed (for e.g., to be used as a proposal distribution within MCMC).

The Riemannian–Gaussian distribution satisfies Assumptions (A3), (A4) and (A5), as seen in Example 4.2 (i). This ensures that the Langevin diffusion converges to its invariant measure exponentially fast. From (5.8) the gradient of  $\phi$  is

$$\nabla\phi(X) = -\frac{\exp_X^{-1}(I)}{\sigma^2} = \frac{X^{1/2}\text{Log}(X)X^{1/2}}{\sigma^2},$$

which grows at infinity as  $x \log x$ ; also note that  $\nabla\phi(I) = 0$ .

---

**Algorithm 5.2** Algorithm to sample from Riemannian–Gaussian distribution on  $\mathcal{P}_3$  with  $O = I_3$ ,  $\sigma = \frac{1}{\sqrt{2}}$  and  $X_0 = \text{hvec}^{-1}((2, 4, 2, 1, 1, 0)^\top)$ .

---

- (1) Input  $h, N$
  - (2) Initialise the chain at  $X_0$  and set  $k = 0$ .
  - (3) Generate  $\xi_k = (\xi_k^1, \xi_k^2, \xi_k^3, \xi_k^4, \xi_k^5, \xi_k^6)^\top$ , where, for every  $k$ ,  $\xi_k^i$  are independent from (3.2).
  - (4) Compute the matrix  $M_k = -\frac{h}{2\sigma^2}\text{Log}(X_k^h) + \sqrt{h}(X_k^h)^{-1/2}\text{hvec}^{-1}(G^{-1/2}(X_k^h)\xi_k)(X_k^h)^{-1/2}$ .
  - (5) Set  $X_{k+1}^h = (X_k^h)^{1/2}\text{Exp}(M_k)(X_k^h)^{1/2}$ .
  - (6) **If**  $k + 1 = N$  **then stop**, **else** put  $k := k + 1$  and **return** to Step 3.
- 

The function  $\varphi : \mathcal{P}_3 \rightarrow \mathbb{R}$  we consider to assess accuracy is  $\varphi(X) = \det(X)$ . The value of  $\mu_\phi(\varphi) \approx 2.11699998$ , evaluated with accuracy of order of  $10^{-8}$  using the function `NIntegrate` in Mathematica. Table 3 and Figure 2 demonstrate that Algorithm 5.2 exhibits the first order convergence.



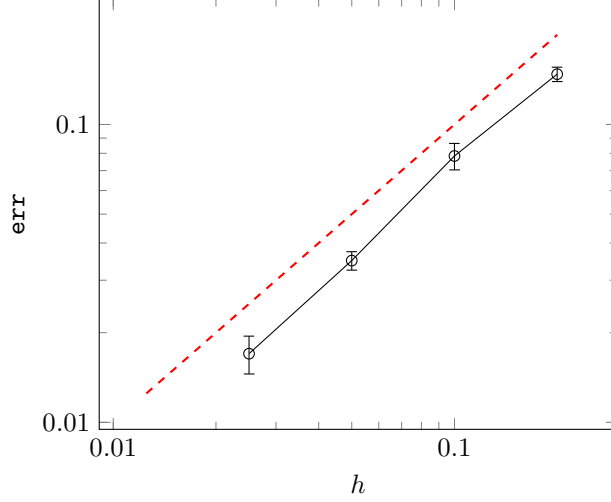


FIGURE 2. Sampling from the Riemannian—Gaussian distribution on  $\mathcal{P}_3$ : log-log plot of the estimation error **err** against  $h$ . Error bars correspond to Monte Carlo error **MCerr**. The reference red line has gradient 1. The parameters for the Riemannian—Gaussian are as in Table 3.

**5.2.2. Distribution with non-convex potential.** Assumption (A5) makes it evident that we need not have log-concavity of the density function to guarantee ergodicity of the SDE. We verify this and demonstrate generality of our algorithm by considering the following distribution with a non-convex potential  $\phi$ :

$$d\mu_\phi = \frac{1}{Z_m} e^{-\phi(X)} d\text{vol}_g, \quad X \in \mathcal{P}_m,$$

where

$$\phi(X) = \rho(X, O)^4 - \rho(X, O)^2,$$

with the normalisation constant  $Z_m$ . This distribution is referred to as one with a double-well potential. Similar to the Riemannian—Gaussian distribution, the constant  $Z_m$  is obtained by evaluating

$$c_m \int_{\mathbb{R}^m} e^{-(\lambda_1^2 + \dots + \lambda_m^2)^2 - [\lambda_1^2 + \dots + \lambda_m^2]} \prod_{i < j} \sinh\left(\frac{|\lambda_i - \lambda_j|}{2}\right) d\lambda_1 \dots d\lambda_m,$$

where  $c_m$  is as in (5.10).

Example 4.2 (ii) verified that  $\phi(X)$  satisfied assumptions (A3), (A4) and (A5). The corresponding Langevin diffusion (2.7) converges exponentially fast to the invariant distribution  $\mu_\phi$ . The gradient takes the form

$$\nabla\phi(X) = -4\rho(X, I_m)^2 \exp_X^{-1}(I_m) + 2 \exp_X^{-1}(I_m) = (4\rho(X, I_m)^2 - 2)X^{1/2}\text{Log}(X)X^{1/2}.$$

We choose  $\varphi(X) = 1/(1 + \text{tr}(X))$  and  $\mu_\phi(\varphi) \approx 0.2204801571878534$ , evaluated with accuracy of order of  $10^{-8}$  using the function **NIntegrate** in Mathematica. Table 4 and Figure 3 show that Algorithm 5.3 exhibits the first order convergence.

---

**Algorithm 5.3** Algorithm to sample from double-well potential distribution on  $\mathcal{P}_3$  with  $O = I_3$  and  $X_0 = \text{hvec}^{-1}((2, 4, 2, 1, 1, 0)^\top)$ .

---

- (1) Input  $h, N$ .
- (2) Initialise the chain at  $X_0$  and set  $k = 0$ .
- (3) Generate  $\xi_k = (\xi_k^1, \xi_k^2, \xi_k^3, \xi_k^4, \xi_k^5, \xi_k^6)^\top$ , where, for every  $k$ ,  $\xi_k^i$  are independent from (3.2).
- (4) Compute the matrix

$$M_k = h(1 - 2\rho(X_k^h, I)^2)\text{Log}(X_k^h) + \sqrt{h}(X_k^h)^{-1/2}\text{hvec}^{-1}(G^{-1/2}(X_k^h)\xi_k)(X_k^h)^{-1/2}.$$

- (5) Set  $X_{k+1}^h = (X_k^h)^{1/2}\text{Exp}(M_k)(X_k^h)^{1/2}$ .
  - (6) **If**  $k + 1 = N$  then **stop**, **else** put  $k := k + 1$  and **return** to Step 3.
- 

$h$	$M$	<b>err</b>	<b>MCerr</b>
0.2	$10^5$	0.00537	0.0003
0.1	$10^5$	0.00162	0.0003
0.05	$10^7$	0.000605	0.00003
0.025	$10^7$	0.000258	0.00003

TABLE 4. The double-well potential distribution. The parameters are  $O = I_m$ ,  $X_0 = \text{hvec}^{-1}((2, 4, 2, 1, 1, 0)^\top)$  and  $T = 5$ .

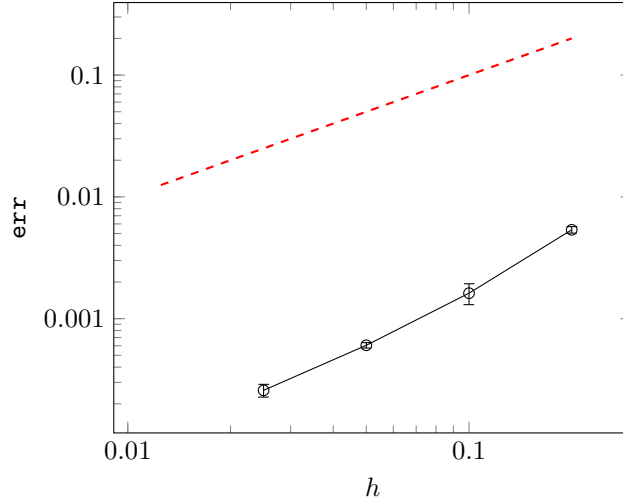


FIGURE 3. Sampling from a distribution with non-convex ‘double-well’ potential on  $\mathcal{P}_3$ : log-log plot of the estimation error **err** against  $h$ . Error bars correspond to Monte Carlo error **MCerr**. The reference red line has gradient 1. The parameters are as in Table 4.

## 6. DISCUSSION AND CONCLUDING REMARKS

In this paper we have studied how the intrinsic Langevin diffusion can be used for sampling on manifolds. To this end we have analyzed and provided theoretical guarantees for an intrinsic Riemannian Langevin algorithm. The algorithm ensures that the corresponding Markov chain moves on the manifold  $M$  without requiring a projection, i.e. it preserves the geometrical features of the corresponding stochastic differential equation. Importantly, we show how the

concept of weak approximations for SDEs in  $\mathbb{R}^q$  and the flat torus  $\mathbb{T}^q$ , and the corresponding proof techniques in deriving weak error bounds, can be transferred to the case of compact Riemannian manifolds. This is a powerful observation which opens the door to carry over the extensive research (conducted by statistical, machine learning, and the numerical analysis communities) on approximation of SDEs in Euclidean spaces to manifolds. For example, sampling from a distribution with compact support on a non-compact manifold, or from a manifold with boundary, are of considerable interest given their practical relevance. These problems are yet to be considered within current literature; only recently has the former been considered even for  $\mathbb{R}^q$  using a reflected diffusion [Leimkuhler et al., 2023]. It is plausible that an intrinsic reflected diffusion can be used to carry out a similar program on manifolds, and this is the subject of our future work.

Next, in this paper we only considered explicit Euler-type schemes. In a similar fashion, we can construct and analyze implicit schemes, second-order sampling algorithms, etc. for Langevin diffusion on manifolds using the arsenal of numerical methods developed in the Euclidean space (see e.g. [Milstein and Tretyakov, 2021]), which potentially can lead to more efficient sampling methods.

Our main interest in this paper is in sampling from a target probability measure which is commonly encountered in statistical applications. It is worth noting the considered algorithm and its analysis are also useful for applications in other research areas, including molecular dynamics, finance, and optimisation. An important example in financial engineering involves multi-factor stochastic volatility models widely used in option pricing and risk analysis, where stochastic modelling of correlation/covariance between factors entering the asset price and volatility processes are of practical value. There is growing interest [Fonseca et al., 2008, Alfonsi et al., 2019] in using a Wishart process [Bru, 1991] to model the time-changing covariance structure, which is an example of stochastic process assuming values in the manifold of positive (semi-)definite matrices. The examples considered in Section 5.2 with the intrinsic approach to modelling stochastic dynamics of positive definite matrices provides a useful, more general class of processes to be used within this context.

#### ACKNOWLEDGEMENTS

The authors were supported by EPSRC grant no. EP/X022617/1. KB acknowledges support from grants EPSRC EP/V048104/1, NSF 2015374 and NIH R37-CA21495.

#### REFERENCES

- A. Abdulle, G. Vilmart, and K.C. Zygalakis. High order numerical approximation of the invariant measure of ergodic SDEs. *SIAM J. Numer. Anal.*, 52:1600–1622, 07 2014.
- P.-A. Absil, R. Mahony, and R. Sepulchre. *Optimization algorithms on matrix manifolds*. Princeton University Press, 2008.
- Au. Alfonsi, D. Krief, and P. Tankov. Long-time large deviations for the multiasset Wishart stochastic volatility model and option pricing. *SIAM J. Finan. Math.*, 10(4):942–976, 2019.
- J. Armstrong and T. King. Curved schemes for stochastic differential equations on, or near, manifolds. *Proceedings Royal Society A*, 478(2262):20210785, 2022.
- T. Aubin. *Some nonlinear problems in Riemannian geometry*. Springer, Berlin, 1998.
- D. Bakry. Un Critère de non-explosion pour certaines diffusions sur une variété Riemannienne complète. *Comptes rendus de l’Académie des sciences. Série 1, Mathématique*, 303:23–26, 1986.
- D. Bakry and M. Émery. Diffusions hypercontractives. In J. Azéma and M. Yor, editors, *Séminaire de Probabilités XIX 1983/84*, pages 177–206. Springer, 1985.

- A. Barp, L. Da Costa, G. Franca, K. Friston, M. Girolami, M.I. Jordan, and G.A. Pavliotis. Geometric methods for sampling, optimisation, inference and adaptive agents. In *Handbook of Statistics*, volume 46, pages 21–78. World Sci., 2022.
- D. J. Best and N. I. Fisher. Efficient simulation of the von Mises distribution. *J. Royal Stat. Society C*, 28(2):152–157, 1979.
- R. L. Bishop and R. J. Crittenden. *Geometry of manifolds*. Academic Press, 2011.
- N. Bou-Rabee and M. Hairer. Non-asymptotic mixing of the MALA algorithm. *IMA J. Numer. Anal.*, 33(1):80–110, 2013.
- M.-F. Bru. Wishart processes. *J. Theor. Probab.*, 4:725–751, 1991.
- J. Cheeger and D.G. Ebin. *Comparison theorems in Riemannian geometry*. North-Holland Publishing Company, 1975.
- X. Cheng, J. Zhang, and S. Sra. Efficient sampling on Riemannian manifolds via Langevin MCMC. In S. Koyejo, S. Mohamed, A. Agarwal, D. Belgrave, K. Cho, and A. Oh, editors, *Advances in neural information processing systems*, volume 35, pages 5995–6006. Curran Associates, Inc., 2022.
- A. S. Dalalyan. Theoretical guarantees for approximate sampling from smooth and log-concave densities. *J. Royal Stat. Society B*, 79(3):651–676, 2017.
- G. Da Prato and J. Zabczyk. *Ergodicity for infinite dimensional systems*. Cambr. Univ. Press, 1996.
- R. L. Davidchack, R. Handel, and M. V. Tretyakov. Langevin thermostat for rigid body dynamics. *J. Chem. Phys.*, 130(23):234101, 2009.
- R. L. Davidchack, T. E. Ouldridge, and M. V. Tretyakov. New Langevin and gradient thermostats for rigid body dynamics. *J. Chem. Phys.*, 142(14):144114, 2015.
- V. De Bortoli, E. Mathieu, M. Hutchinson, J. Thornton, Y. W. Teh, and A. Doucet. Riemannian score-based generative modelling. In S. Koyejo, S. Mohamed, A. Agarwal, D. Belgrave, K. Cho, and A. Oh, editors, *Advances in Neural Information Processing Systems*, volume 35, pages 2406–2422. Curran Associates, Inc., 2022.
- T. D. Downs. Orientation statistics. *Biometrika*, 59(3):665–676, 1972.
- A. Durmus and É. Moulines. Nonasymptotic convergence analysis for the unadjusted Langevin algorithm. *Ann. Appl. Probab.*, 27(3):1551 – 1587, 2017.
- K. D. Elworthy. *Stochastic differential equations on manifolds*. London Mathematical Society Lecture Note Series. Cambridge University Press, 1982.
- B. Everitt and C. Maclachlan. Constructing hyperbolic manifolds. *Computational and Geometric Aspects of Modern Algebra. Michael Atkinson et al.(Editors), London Maths. Soc. Lect. Notes*, 275:78–86, 2000.
- J. Da Fonseca, M. Grasselli, and C. Tebaldi. A multifactor volatility Heston model. *Quant. Finance*, 8(6):591–604, 2008.
- M. Freidlin. *Functional integration and partial differential equations*. Princeton Univ. Press, 1985.
- S. Gallot, D. Hulin, and J. Lafontaine. *Riemannian geometry*, volume 2. Springer, 1990.
- K. Gasmiriy and S. S. Vempala. Convergence of the Riemannian Langevin algorithm. *arXiv:2204.10818*, 2022.
- M. Girolami and B. Calderhead. Riemann manifold Langevin and Hamiltonian Monte Carlo methods. *J. Royal Stat. Society B*, 73(2):123–214, 2011.
- R. E. Greene and H.-H. Wu. *Function theory on manifolds which possess a pole*. Springer, 2006.
- E. Hairer, S. P. Nørsett, and G. Wanner. *Solving ordinary differential equations. I. Nonstiff problems*. Springer, Berlin, 1993.

- E. Hairer, C. Lubich, and G. Wanner. *Geometric numerical integration: structure preserving algorithms for ordinary differential equations*. Springer, Berlin, 2002.
- E. P. Hsu. *Stochastic analysis on manifolds*. Amer. Math. Soc., 2002.
- C.-W. Huang, M. Aghajohari, J. Bose, P. Panangaden, and A. C. Courville. Riemannian diffusion models. In S. Koyejo, S. Mohamed, A. Agarwal, D. Belgrave, K. Cho, and A. Oh, editors, *Advances in Neural Information Processing Systems*, volume 35, pages 2750–2761. Curran Associates, Inc., 2022.
- M. Hutzenthaler and A. Jentzen. *Numerical approximations of stochastic differential equations with non-globally Lipschitz continuous coefficients*, volume 236 of *Mem. Amer. Math. Soc.* AMS, Providence, 2015.
- M. Hutzenthaler, A. Jentzen, and P. E. Kloeden. Strong and weak divergence in finite time of Euler’s method for stochastic differential equations with non-globally Lipschitz continuous coefficients. *Proc. R. Soc. A*, 467:1563–1576, 2011.
- K. Ichihara. Curvature, geodesics and the Brownian motion on a Riemannian manifold i—recurrence properties. *Nagoya Math. J.*, 87:101–114, 1982a.
- K. Ichihara. Curvature, geodesics and the Brownian motion on a Riemannian manifold ii—explosion properties. *Nagoya Math. J.*, 87:115–125, 1982b.
- N. Ikeda and S. Watanabe. *Stochastic differential equations and diffusion processes*. Elsevier, 2014.
- J. Jost. *Riemannian geometry and geometric analysis*. Universitext. Springer, 2008.
- P. E. Jupp and K. V. Mardia. Maximum likelihood estimators for the matrix von Mises-Fisher and Bingham distributions. *Ann. Statistics*, 7(3):599–606, 1979.
- W. S. Kendall. Brownian motion on a surface of negative curvature. *Séminaire de probabilités de Strasbourg*, 18:70–76, 1984.
- R. Khasminskii. *Stochastic stability of differential equations*. Springer, 2012.
- S. Kobayashi and K. Nomizu. *Foundations of differential geometry, vol II*. John Wiley & Sons, 1969.
- O. A. Ladyzhenskaya, V. A. Solonnikov, and N. N. Ural’tseva. *Linear and quasi-linear equations of parabolic type*, volume 23 of *Trans. Math. Monog.* Amer. Math. Soc., Providence, RI, 1968.
- A. Laurent and G. Vilmart. Order conditions for sampling the invariant measure of ergodic stochastic differential equations on manifolds. *Found. Comput. Math.*, 22:649–695, 2022.
- B. Leimkuhler and C. Matthews. *Molecular dynamics with deterministic and stochastic numerical methods*. Springer, Berlin, 2015.
- B. Leimkuhler, A. Sharma, and M. V. Tretyakov. Simplest random walk for approximating Robin boundary value problems and ergodic limits of reflected diffusions. *Ann. Appl. Probab.*, 33(3):1904 – 1960, 2023.
- T. Lelièvre, M. Rousset, and G. Stoltz. Langevin dynamics with constraints and computation of free energy differences. *Mathem. Computation*, 81(280):2071–2125, 2012.
- A. Lewis. *Contributions to Stein’s method on Riemannian manifolds*. PhD thesis, University of Nottingham, 2023.
- X.-M. Li. *Stochastic flows on non-compact manifolds*. PhD thesis, University of Warwick, 1992.
- A. Lunardi. *Analytic semigroups and optimal regularity in parabolic problems*. Springer, 1995.
- S. J. A. Malham and A. Wiese. Stochastic Lie group integrators. *SIAM J. Scien. Comput.*, 30(2):597–617, 2008.
- O. Mangoubi and A. Smith. Rapid mixing of geodesic walks on manifolds with positive curvature. *Ann. Appl. Probab.*, 28(4):2501–2543, 2018.

- J. Mattingly, A. Stuart, and M. V. Tretyakov. Convergence of numerical time-averaging and stationary measures via Poisson equations. *SIAM J. Numer. Anal.*, 48(2):552–577, 2010.
- J. C. Mattingly, A. M. Stuart, and D. J. Higham. Ergodicity for SDEs and approximations: locally Lipschitz vector fields and degenerate noise. *Stoch. Proc. Appl.*, 101:185–232, 2002.
- J. H. Mentink, M. V. Tretyakov, A. Fasolino, M. I. Katsnelson, and Th. Rasing. Stable and fast semi-implicit integration of the stochastic Landau-Lifshitz equation. *J. Phys.: Condens. Matter*, 22(17):176001, 2010.
- G. N. Milstein and M. V. Tretyakov. Numerical integration of stochastic differential equations with nonglobally Lipschitz coefficients. *SIAM J. Numer. Anal.*, 43(3):1139–1154, 2005.
- G. N. Milstein and M. V. Tretyakov. Computing ergodic limits for Langevin equations. *Physica D*, 229(1):81–95, 2007.
- G. N. Milstein and M. V. Tretyakov. *Stochastic numerics for mathematical physics*. Springer, 2nd edition, 2021.
- C. Miranda. *Partial differential equations of elliptic type*. Springer, 1969.
- M. Moakher and M. Zérai. The Riemannian geometry of the space of positive-definite matrices and its application to the regularization of positive-definite matrix-valued data. *J. Mathem. Imaging and Vision*, 40:171–187, 2011.
- L. I. Nicolaescu. *Lectures on the geometry of manifolds*. World Scientific, 2007.
- X. Pennec, P. Fillard, and N. Ayache. A Riemannian framework for tensor computing. *Inter. J. Computer Vision*, 66:41–66, 2006.
- G. O. Roberts and R. L. Tweedie. Exponential convergence of Langevin distributions and their discrete approximations. *Bernoulli*, 2:341–363, 1996.
- S. Said, L. Bombrun, Y. Berthoumieu, and J. H. Manton. Riemannian Gaussian distributions on the space of symmetric positive definite matrices. *IEEE Transactions on Information Theory*, 63:2153–2170, 2017.
- K. Sato, A. Takeda, R. Kawai, and T. Suzuki. Convergence error analysis of reflected gradient Langevin dynamics for globally optimizing non-convex constrained problems. *arXiv:2203.10215*, 2022.
- U. Sharma and W. Zhang. Nonreversible sampling schemes on submanifolds. *SIAM J. Numer. Anal.*, 59(6):2989–3031, 2021.
- D. Talay. Second-order discretization schemes of stochastic differential systems for the computation of the invariant law. *Stoch. Stoch. Reports*, 29:13–36, 1990.
- Y. W. Teh, A. H. Thiery, and S. J. Vollmer. Consistency and fluctuations for stochastic gradient Langevin dynamics. *J. Machine Learning Research*, 17(7):1–33, 2016.
- M. V. Tretyakov and Z. Zhang. A fundamental mean-square convergence theorem for SDEs with locally Lipschitz coefficients and its applications. *SIAM J. Numer. Anal.*, 51:3135–3162, 2013.
- F.-Y. Wang. Log-Sobolev inequalities: different roles of Ric and Hess. *Ann. Probab.*, 37(4):1587–1604, 2009.
- F.-Y. Wang. *Analysis for diffusion processes on Riemannian manifolds*. World Scientific, 2013.
- X. Wang, Q. Lei, and I. Panageas. Fast convergence of Langevin dynamics on manifold: Geodesics meet log-sobolev. *Advances in Neural Information Processing Systems*, 33:18894–18904, 2020.
- G. S. Watson. Equatorial distributions on a sphere. *Biometrika*, 52(1/2):193–201, 1965.
- A. T. A. Wood. Simulation of the von Mises Fisher distribution. *Commun. Statistics-Simulation Comput.*, 23(1):157–164, 1994.

## APPENDIX A. PROOFS

In this section we prove the three theorems stated in Section 3. Recall that Theorem 3.1 gives an error estimate for the ensemble-averaging estimator  $\hat{\mu}_{\phi,N}(\varphi)$  of  $\mu_\phi(\varphi)$ , it is proved in Section A.1 exploiting the backward Kolmogorov PDE (cf. similar approach in the case of SDEs in  $\mathbb{R}^q$  in Talay [1990]). Theorem 3.2 on dependence of bias and variance of the time-averaging estimator  $\tilde{\mu}_{\phi,N}(\varphi)$  on  $h$  and  $T$  is proved in Section A.2 exploiting the Poisson PDE (cf. similar approach for SDEs on torus in Mattingly et al. [2010] and for reflected SDEs in Leimkuhler et al. [2023]). Theorem 3.3 shows closeness of the invariant measure of the solution  $X(t)$  of the SDEs (2.7) and an invariant measure of the Markov chain  $X_n^h$  from (3.3), it is proved in Section A.3.

Since the covariant Taylor's expansion plays a major role in the proofs of Theorems 3.1 and 3.2, we state it here. Let  $f \in C^4(M)$  taking values in  $\mathbb{R}$  and the geodesic curve  $\gamma(s)$ ,  $s \in \mathbb{R}$  on  $M$ , be so that  $\gamma(0) = x$  and  $\dot{\gamma}(0) = V$ . Introduce  $F(s) := f(\gamma(s)) : \mathbb{R} \rightarrow \mathbb{R}$  for which Taylor's expansion can be written as

$$(A.1) \quad F(s) = F(0) + s \frac{d}{ds} F(0) + \frac{s^2}{2} \frac{d^2}{ds^2} F(0) + \frac{s^3}{6} \frac{d^3}{ds^3} F(0) + \frac{s^4}{24} \frac{d^4}{ds^4} F(\alpha),$$

where  $\alpha \in (0, s)$ . Taking into account that  $\gamma$  is a geodesic, one can show that

$$(A.2) \quad \begin{aligned} f(\gamma(s)) &= f(\gamma(0)) + s Df(\gamma(0))(\dot{\gamma}(0)) + \frac{s^2}{2} D^2 f(\gamma(0))(\dot{\gamma}(0), \dot{\gamma}(0)) \\ &\quad + \frac{s^3}{6} D^3 f(\gamma(0))(\dot{\gamma}(0), \dot{\gamma}(0), \dot{\gamma}(0)) + \frac{s^4}{24} D^4 f(\gamma(\alpha))(\dot{\gamma}(\alpha), \dot{\gamma}(\alpha), \dot{\gamma}(\alpha), \dot{\gamma}(\alpha)) \\ &= f(x) + s Df(x)(V) + \frac{s^2}{2} D^2 f(x)(V, V) + \frac{s^3}{6} D^3 f(x)(V, V, V) \\ &\quad + \frac{s^4}{24} D^4 f(\gamma(\alpha))(\dot{\gamma}(\alpha), \dot{\gamma}(\alpha), \dot{\gamma}(\alpha), \dot{\gamma}(\alpha)). \end{aligned}$$

**A.1. Proof of Theorem 3.1.** For brevity, we denote  $u(t, x)$  as  $u$ ,  $\frac{\partial u}{\partial t}(t, x)$  as  $\frac{\partial u}{\partial t}$ ,  $\nabla u(t, x)$  as  $\nabla u$ ,  $Du(t, x)$  as  $Du$ ,  $D^k u(t, x)$  as  $D^k u$ ,  $\nabla \phi(x)$  as  $\nabla \phi$ ,  $g^{-1/2}(x)$  as  $g^{-1/2}$  and  $u(t_n, X_n^h)$  as  $u_n$ ,  $n = 0, \dots, N-1$ , where  $u(t, x)$  is the solution of (2.12) and  $\phi(x)$  is from (2.7).

We need the following one-step approximation lemma to prove Theorem 3.1.

**Lemma A.1** (One-step approximation lemma). *Let Assumptions (A1) and (A2) and  $\varphi \in C^{4,\epsilon}(M)$  hold. Given  $x \in M$ , let  $X_1^h$  be computed according to (3.3), i.e.,*

$$(A.3) \quad X_1^h = \exp_x \left( -\frac{h}{2} \nabla \phi(x) + h^{1/2} g^{-1/2}(x) \xi \right).$$

Then

$$(A.4) \quad \mathbb{E}[u(t+h, X_1^h) - u(t, x)] \leq C h^2 e^{-\lambda(T-t)},$$

where  $C > 0$  is independent of  $T$  and  $h$  and it linearly depends on  $\|\varphi\|_{C^{4,\epsilon}(M)}$  but otherwise is independent of  $\varphi$ .

*Proof.* Define  $\gamma$  to be the geodesic with initial conditions

$$(A.5) \quad \gamma(0) = x,$$

$$(A.6) \quad \dot{\gamma}(0) = V := -\frac{h^{1/2}}{2} \nabla \phi + g^{-1/2} \xi.$$

Then, we can write  $\gamma(s) = \exp_x(sV)$ . Clearly,  $\gamma(\sqrt{h}) = X_1^h$ .

Applying the Taylor expansion to  $u(t+h, \gamma(s))$  around  $t$ , we obtain

$$(A.7) \quad u(t+h, \gamma(s)) = u(t, \gamma(s)) + h \frac{\partial u}{\partial t}(t, \gamma(s)) + \frac{h^2}{2} \frac{\partial^2 u}{\partial t^2}(t(\alpha_1), \gamma(s)),$$

where  $t(\alpha_1) := t + \alpha_1 h \in (t, t+h)$  since  $\alpha_1 \in (0, 1)$ .

Applying the covariant Taylor series (see (A.2)) to the function  $u(t, \gamma(s))$  along the geodesic  $\gamma$ , we get

$$(A.8) \quad \begin{aligned} u(t, \gamma(s)) &= u + sDu(V) + \frac{s^2}{2} D^2u(V, V) + \frac{s^3}{6} D^3u(V, V, V) \\ &\quad + \frac{s^4}{24} D^4u(t, \gamma(\alpha_2))(\dot{\gamma}(\alpha_2), \dot{\gamma}(\alpha_2), \dot{\gamma}(\alpha_2), \dot{\gamma}(\alpha_2)), \end{aligned}$$

where  $\alpha_2 \in (0, \sqrt{h})$ . Similarly we obtain

$$(A.9) \quad \frac{\partial u}{\partial t}(t, \gamma(s)) = \frac{\partial u}{\partial t} + sD \frac{\partial u}{\partial t}(V) + \frac{s^2}{2} D^2 \frac{\partial u}{\partial t}(t, \gamma(\alpha_3))(\dot{\gamma}(\alpha_3), \dot{\gamma}(\alpha_3)),$$

where  $\alpha_3 \in (0, \sqrt{h})$ .

Substituting (A.8) and (A.9) in (A.7), we arrive at

$$(A.10) \quad \begin{aligned} u(t+h, \gamma(s)) &= u + h \frac{\partial u}{\partial t} + sDu(V) + \frac{s^2}{2} D^2u(V, V) \\ &\quad + \frac{s^3}{6} D^3u(V, V, V) + \frac{s^4}{24} D^4u(t, \gamma(\alpha_2))(\dot{\gamma}(\alpha_2), \dot{\gamma}(\alpha_2), \dot{\gamma}(\alpha_2), \dot{\gamma}(\alpha_2)) \\ &\quad + hsD \frac{\partial u}{\partial t}(V) + h \frac{s^2}{2} D^2 \frac{\partial u}{\partial t}(t, \gamma(\alpha_3))(\dot{\gamma}(\alpha_3), \dot{\gamma}(\alpha_3)) + \frac{h^2}{2} \frac{\partial^2 u}{\partial t^2}(t(\alpha_1), \gamma(s)). \end{aligned}$$

Taking expectation on both sides and putting  $s = \sqrt{h}$ , we get

$$(A.11) \quad \begin{aligned} \mathbb{E}(u(t+h, X_1^h)) &= u + h \frac{\partial u}{\partial t} + \mathbb{E} \left( h^{1/2} Du(V) + \frac{h}{2} D^2u(V, V) \right. \\ &\quad + \frac{h^{3/2}}{6} D^3u(V, V, V) + \frac{h^2}{24} D^4u(t, \gamma(\alpha_2))(\dot{\gamma}(\alpha_2), \dot{\gamma}(\alpha_2), \dot{\gamma}(\alpha_2), \dot{\gamma}(\alpha_2)) \\ &\quad \left. + h^{3/2} D \frac{\partial u}{\partial t}(V) + \frac{h^2}{2} D^2 \frac{\partial u}{\partial t}(t, \gamma(\alpha_3))(\dot{\gamma}(\alpha_3), \dot{\gamma}(\alpha_3)) + \frac{h^2}{2} \frac{\partial^2 u}{\partial t^2}(t(\alpha_1), \gamma(s)) \right). \end{aligned}$$

Denote  $i$ -th component of  $V$  as  $V^i$ , i.e.  $V^i = \left( -\frac{h^{1/2}}{2} \nabla \phi + g^{-1/2} \xi \right)^i$ . Using the properties of the random variables  $\xi^i$

$$(A.12) \quad \mathbb{E}[\xi^i] = 0, \quad \mathbb{E}[\xi^i \xi^j] = \delta_{ij}, \quad \mathbb{E}[\xi^i \xi^j \xi^k] = 0, \quad \mathbb{E}[(\xi^i)^2 (\xi^j)^2] = 1 \text{ for } i \neq j,$$

we deduce that

$$\begin{aligned} \mathbb{E}(V^i V^j V^k) &= -\frac{h^{3/2}}{8} (\nabla \phi)^i (\nabla \phi)^j (\nabla \phi)^k + \frac{3h}{4} (\nabla \phi)^i (\nabla \phi)^j \mathbb{E}((g^{-1/2} \xi)^k) \\ &\quad - \frac{3h^{1/2}}{2} (\nabla \phi)^i \mathbb{E}((g^{-1/2} \xi)^j (g^{-1/2} \xi)^k) + \mathbb{E}((g^{-1/2} \xi)^i (g^{-1/2} \xi)^j (g^{-1/2} \xi)^k) \\ &= -\frac{h^{3/2}}{8} (\nabla \phi)^i (\nabla \phi)^j (\nabla \phi)^k - \frac{3h^{1/2}}{2} (\nabla \phi)^i \mathbb{E}((g^{1/2})^{jl} \xi_l (g^{1/2})^{km} \xi_m) \\ &= -\frac{h^{3/2}}{8} (\nabla \phi)^i (\nabla \phi)^j (\nabla \phi)^k - \frac{3h^{1/2}}{2} (\nabla \phi)^i (g^{1/2})^{jl} (g^{1/2})^{km} \delta_{lm} \end{aligned}$$



$$(A.13) \quad = -\frac{h^{3/2}}{8}(\nabla\phi)^i(\nabla\phi)^j(\nabla\phi)^k - \frac{3h^{1/2}}{2}(\nabla\phi)^i g^{jk},$$

where  $i, j, k = 1, \dots, q$  and  $\delta_{ij}$  is the Kronecker delta. Further, we have

$$(A.14) \quad \begin{aligned} \mathbb{E}(h^{1/2}Du(V)) &= -\frac{h}{2}g(\nabla\phi, \nabla u), \\ \mathbb{E}(hD^2u(V, V)) &= h\mathbb{E}(\text{Hess}^u(g^{-1/2}\xi, g^{-1/2}\xi)) + \frac{h^2}{4}D^2u(\nabla\phi, \nabla\phi) \\ &= h\mathbb{E}(\text{Hess}_{ij}^u(g^{-1/2}\xi)^i(g^{-1/2}\xi)^j) + \frac{h^2}{4}D^2u(\nabla\phi, \nabla\phi) \\ &= h\mathbb{E}(\text{Hess}_{ij}^u(g^{1/2})^{ik}\xi_k(g^{1/2})^{jl}\xi_l) + \frac{h^2}{4}D^2u(\nabla\phi, \nabla\phi) \\ &= h\text{Hess}_{ij}^u(g^{1/2})^{ik}(g^{1/2})^{jl}\delta_{kl} + \frac{h^2}{4}D^2u(\nabla\phi, \nabla\phi) \\ &= h\text{Hess}_{ij}^u g^{ij} + \frac{h^2}{4}D^2u(\nabla\phi, \nabla\phi) \\ (A.15) \quad &= h\Delta_M u + \frac{h^2}{4}D^2u(\nabla\phi, \nabla\phi), \end{aligned}$$

$$(A.16) \quad \begin{aligned} \mathbb{E}\left(h^{3/2}D^3u(V, V, V)\right) &= h^{3/2}D^3u(\partial_i, \partial_j, \partial_k)\mathbb{E}(V^i V^j V^k) \\ &= -\frac{h^3}{8}D^3u(\partial_i, \partial_j, \partial_k)(\nabla\phi)^i(\nabla\phi)^j(\nabla\phi)^k \\ &\quad - \frac{3h^2}{2}D^3u(\partial_i, \partial_j, \partial_k)(\nabla\phi)^i g^{jk}, \end{aligned}$$

$$(A.17) \quad \mathbb{E}\left(h^{3/2}D\frac{\partial u}{\partial t}(V)\right) = h^{3/2}D\frac{\partial u}{\partial t}(\partial_i)\mathbb{E}(V^i) = \frac{h^2}{2}D\frac{\partial u}{\partial t}(\partial_i)(\nabla\phi)^i.$$

Substituting (A.14)-(A.17) in (A.11), we get

$$(A.18) \quad \begin{aligned} \mathbb{E}(u(t+h, X_1^h)) &= u + h\frac{\partial u}{\partial t} - \frac{h}{2}g(\nabla\phi, \nabla u) + \frac{h}{2}\Delta_M u \\ &\quad + \frac{h^2}{8}D^2u(\nabla\phi, \nabla\phi) - \frac{h^3}{48}D^3u(\partial_i, \partial_j, \partial_k)(\nabla\phi)^i(\nabla\phi)^j(\nabla\phi)^k \\ &\quad - \frac{h^2}{4}D^3u(\partial_i, \partial_j, \partial_k)(\nabla\phi)^i g^{jk} + \frac{h^2}{2}D\frac{\partial u}{\partial t}(\partial_i)(\nabla\phi)^i \\ &\quad + \mathbb{E}\left(\frac{h^2}{24}D^4u(t, \gamma(\alpha_2))(\dot{\gamma}(\alpha_2), \dot{\gamma}(\alpha_2), \dot{\gamma}(\alpha_2), \dot{\gamma}(\alpha_2))\right. \\ &\quad \left.+ \frac{h^2}{2}D^2\frac{\partial u}{\partial t}(t, \gamma(\alpha_3))(\dot{\gamma}(\alpha_3), \dot{\gamma}(\alpha_3)) + \frac{h^2}{2}\frac{\partial^2 u}{\partial t^2}(t(\alpha_1), \gamma(s))\right). \end{aligned}$$

We note that the remainder terms include a linear combination of derivatives of  $u$  which can be estimated using Assumption (A2) together with boundedness of  $\nabla\phi$  thanks to compactness of  $M$  and Assumption (A1). Consequently, we arrive at (A.4).  $\square$

**Proof of Theorem 3.1.** Using (2.12) and (2.14), we can write

$$\begin{aligned} |\mathbb{E}(\varphi(X_N^h)) - \mu_\phi(\varphi)| &\leq |\mathbb{E}(\varphi(X_N^h)) - \mathbb{E}(\varphi(X(T)))| + |\mathbb{E}(\varphi(X(T))) - \mu_\phi(\varphi)| \\ &= |\mathbb{E}(u(t_N, X_N^h)) - u(0, x_0)| + |\mathbb{E}(\varphi(X(T))) - \mu_\phi(\varphi)| \end{aligned}$$

$$= \left| \mathbb{E} \left( \sum_{n=0}^{N-1} \mathbb{E} \left( u_{n+1} - u_n \mid X_n^h \right) \right) \right| + |\mathbb{E}(\varphi(X(T))) - \mu_\phi(\varphi)|.$$

Using Lemma A.1 and (2.11), we get

$$|\mathbb{E}(\varphi(X_N^h)) - \mu_\phi(\varphi)| \leq C \sum_{n=0}^{N-1} e^{-\lambda(T-t_n)} + Ce^{-\lambda T} \leq C(h + e^{-\lambda T}),$$

where  $C > 0$  is a constant independent of  $h$  and  $T$  and it linearly depends on  $\|\varphi\|_{C^{4,\epsilon}(M)}$  but otherwise  $C, \lambda$  are independent of  $\varphi$ .  $\square$

**A.2. Proof of Theorem 3.2.** For this section, let us denote  $u_n := u(X_n^h)$ ,  $\nabla\phi_n := \nabla\phi(X_n^h)$ ,  $g_n^{-1/2} = g^{-1/2}(X_n^h)$  and  $V_n = -\frac{h^{1/2}}{2}\nabla\phi_n + g_n^{-1/2}\xi_{n+1}$ , where  $u(x)$  is the solution of (2.15).

*Proof.* Define  $\gamma_{V_n}$  to be the geodesic with initial conditions

$$(A.19) \quad \gamma_{V_n}(0) = X_n^h,$$

$$(A.20) \quad \dot{\gamma}_{V_n}(0) = V_n := -\frac{h^{1/2}}{2}\nabla\phi_n + g_n^{-1/2}\xi_{n+1}.$$

Applying the covariant Taylor expansion (A.2) with  $s = \sqrt{h}$  to  $u_{n+1}$  around  $X_n^h$ , we obtain

$$(A.21) \quad \begin{aligned} u_{n+1} - u_n &= h^{1/2}Du_n(V_n) + \frac{h}{2}D^2u_n(V_n, V_n) \\ &+ \frac{h^{3/2}}{6}D^3u_n(V_n, V_n, V_n) + \frac{h^2}{24}D^4u(\gamma_{V_n}(\alpha))(\dot{\gamma}_{V_n}(\alpha), \dot{\gamma}_{V_n}(\alpha), \dot{\gamma}_{V_n}(\alpha), \dot{\gamma}_{V_n}(\alpha)), \end{aligned}$$

where  $\alpha \in (0, \sqrt{h})$ . Taking expectation conditioned on  $X_n^h$ , we get

$$(A.22) \quad \begin{aligned} \mathbb{E}(u_{n+1} \mid X_n^h) &= u_n - \frac{h}{2}g(\nabla\phi_n, \nabla u_n) + \frac{h}{2}\Delta_M u_n \\ &+ \frac{h^2}{8}D^2u_n(\nabla\phi_n, \nabla\phi_n) - \frac{h^3}{48}D^3u_n(\partial_i, \partial_j, \partial_k)(\nabla\phi_n)^i(\nabla\phi_n)^j(\nabla\phi_n)^k \\ &- \frac{h^2}{2}D^3u_n(\partial_i, \partial_j, \partial_k)(\nabla\phi_n)^i g_n^{jk} \\ &+ \frac{h^2}{24}\mathbb{E}[D^4u(\gamma_{V_n}(\alpha))(\dot{\gamma}_{V_n}(\alpha), \dot{\gamma}_{V_n}(\alpha), \dot{\gamma}_{V_n}(\alpha), \dot{\gamma}_{V_n}(\alpha)) \mid X_n^h], \end{aligned}$$

where  $\partial_i$ ,  $i = 1, \dots, q$ , denote basis vectors of  $T_{X_n^h}M$ . The arguments employed to obtain (A.22) are based on (A.14)-(A.16) except that here we take expectation conditional on  $X_n^h$  and  $u$  represents the solution of the Poisson PDE (2.15). Rearranging (A.22) and using the Poisson PDE (2.15), we arrive at

$$(A.23) \quad \begin{aligned} h\varphi(X_n^h) - h\mu_\phi(\varphi) &= \mathbb{E}(u_{n+1} \mid X_n^h) - u_n - \frac{h^2}{8}D^2u_n(\nabla\phi_n, \nabla\phi_n) \\ &+ \frac{h^3}{48}D^3u_n(\partial_i, \partial_j, \partial_k)(\nabla\phi_n)^i(\nabla\phi_n)^j(\nabla\phi_n)^k \\ &+ \frac{h^2}{2}D^3u_n(\partial_i, \partial_j, \partial_k)(\nabla\phi_n)^i g_n^{jk} \\ &- \frac{h^2}{24}\mathbb{E}[D^4u(\gamma_{V_n}(\alpha))(\dot{\gamma}_{V_n}(\alpha), \dot{\gamma}_{V_n}(\alpha), \dot{\gamma}_{V_n}(\alpha), \dot{\gamma}_{V_n}(\alpha)) \mid X_n^h]. \end{aligned}$$

Taking expectation on both sides, summing over  $n = 0, \dots, N-1$ , and applying (2.16), we ascertain

$$\left| h\mathbb{E} \sum_{n=0}^{N-1} \varphi(X_n^h) - hN\mu_\phi(\varphi) \right| \leq |\mathbb{E}(u_N - u_0)| + Ch^2N,$$

where  $C > 0$  is independent of  $T$  and  $h$  and it linearly depends on  $\|\varphi\|_{C^{2,\epsilon}(M)}$  but otherwise it is independent of  $\varphi$ . Dividing by  $T$  (note that  $T = Nh$ ) gives us the result stated in (3.15):

$$|\mathbb{E}\tilde{\mu}_{\phi,N}(\varphi) - \mu_\phi(\varphi)| \leq C\left(h + \frac{1}{T}\right),$$

where we have used the fact that  $|u_N - u_0|$  is bounded uniformly in  $x$  due to compactness of the manifold  $M$  and  $u(x) \in C^{4,\epsilon}(M)$ .

To show the bound (3.16), we start with (A.21)

$$\begin{aligned} u_{n+1} - u_n &= h\mathcal{A}u_n + h^{1/2}Du_n(g_n^{-1/2}\xi_{n+1}) + \frac{h}{2}\left(D^2u_n(V_n, V_n) - \Delta_M u_n\right) \\ (A.24) \quad &+ \frac{h^{3/2}}{6}D^3u_n(V_n, V_n, V_n) + \frac{h^2}{24}D^4u(\gamma_{V_n}(\alpha))(\dot{\gamma}_{V_n}(\alpha), \dot{\gamma}_{V_n}(\alpha), \dot{\gamma}_{V_n}(\alpha), \dot{\gamma}_{V_n}(\alpha)). \end{aligned}$$

We rearrange (A.24), sum over  $n = 0, \dots, N-1$  and use (2.15) to arrive at

$$\begin{aligned} Nh(\tilde{\mu}_{\phi,N}(\varphi) - \mu_\phi(\varphi)) &= u_N - u_0 \\ &+ \sum_{n=0}^{N-1} \left( -h^{1/2}Du_n(g_n^{-1/2}\xi_{n+1}) - \frac{h}{2}\left(D^2u_n(V_n, V_n) - \Delta_M u_n\right) \right. \\ &- \frac{h^{3/2}}{6}D^3u_n(V_n, V_n, V_n) \\ (A.25) \quad &- \left. \frac{h^2}{24}D^4u(\gamma_{V_n}(\alpha))(\dot{\gamma}_{V_n}(\alpha), \dot{\gamma}_{V_n}(\alpha), \dot{\gamma}_{V_n}(\alpha), \dot{\gamma}_{V_n}(\alpha)) \right). \end{aligned}$$

Squaring both sides and dividing by  $T^2$ , we obtain

$$\begin{aligned} (\tilde{\mu}_{\phi,N}(\varphi) - \mu_\phi(\varphi))^2 &\leq \frac{C}{T^2}(u_N - u_0)^2 + \frac{Ch}{T^2}\left(\sum_{n=0}^{N-1} Du_n(g_n^{-1/2}\xi_{n+1})\right)^2 \\ &+ \frac{CNh^4}{T^2}\sum_{n=0}^{N-1} (D^2u_n(\nabla\phi_n, \nabla\phi_n))^2 \\ &+ \frac{Ch^3}{T^2}\left(\sum_{n=0}^{N-1} D^2u_n(g_n^{-1/2}\xi_{n+1}, \nabla\phi_n)\right)^2 \\ &+ \frac{Ch^3}{T^2}\left(\sum_{n=0}^{N-1} D^2u_n(\nabla\phi_n, g_n^{-1/2}\xi_{n+1})\right)^2 \\ &+ \frac{Ch^2}{T^2}\left(\sum_{n=0}^{N-1} D^2u_n(g_n^{-1/2}\xi_{n+1}, g_n^{-1/2}\xi_{n+1}) - \Delta_M u_n\right)^2 \\ &+ \frac{CNh^6}{T^2}\sum_{n=0}^{N-1} (D^3u_n(\nabla\phi_n, \nabla\phi_n, \nabla\phi_n))^2 \end{aligned}$$

$$\begin{aligned}
& + \frac{CNh^5}{T^2} \sum_{n=0}^{N-1} (D^3 u_n(\partial_i, \partial_j, \partial_k)(\nabla \phi)^i(\nabla \phi)^j(g_n^{-1/2} \xi_{n+1})^k)^2 \\
& + \frac{CNh^4}{T^2} \sum_{n=0}^{N-1} (D^3 u_n(\partial_i, \partial_j, \partial_k)(\nabla \phi)^i(g_n^{-1/2} \xi_{n+1})^j(g_n^{-1/2} \xi_{n+1})^k)^2 \\
& + \frac{Ch^3}{T^2} \left( \sum_{n=0}^{N-1} D^3 u_n(\partial_i, \partial_j, \partial_k)(g_n^{-1/2} \xi_{n+1})^i(g_n^{-1/2} \xi_{n+1})^j(g_n^{-1/2} \xi_{n+1})^k \right)^2 \\
& + \frac{CNh^4}{T^2} \sum_{n=0}^{N-1} (D^4 u(\gamma_{V_n}(\alpha))(\dot{\gamma}_{V_n}(\alpha), \dot{\gamma}_{V_n}(\alpha), \dot{\gamma}_{V_n}(\alpha), \dot{\gamma}_{V_n}(\alpha)))^2.
\end{aligned}
\tag{A.26}$$

Using (A.12), we get

$$\begin{aligned}
\mathbb{E} \left( \sum_{n=0}^{N-1} Du_n(g_n^{-1/2} \xi_{n+1}) \right)^2 &= \sum_{n=0}^{N-1} \mathbb{E}(Du_n(g_n^{-1/2} \xi_{n+1}))^2 \\
&+ 2 \sum_{k < n} \mathbb{E}(Du_k(g_k^{-1/2} \xi_{k+1}) Du_n(g_n^{-1/2} \xi_{n+1})) \\
&= \sum_{n=0}^{N-1} \mathbb{E}(Du_n(g_n^{-1/2} \xi_{n+1}))^2,
\end{aligned}
\tag{A.27}$$

and

$$\mathbb{E} \left( \sum_{n=0}^{N-1} D^2 u_n(g_n^{-1/2} \xi_{n+1}, \nabla \phi_n) \right)^2 = \sum_{n=0}^{N-1} \mathbb{E}(D^2 u_n(g_n^{-1/2} \xi_{n+1}, \nabla \phi_n))^2.
\tag{A.28}$$

Analogously,

$$\begin{aligned}
& \mathbb{E} \left( \sum_{n=0}^{N-1} D^3 u_n(\partial_i, \partial_j, \partial_k)(g_n^{-1/2} \xi_{n+1})^i(g_n^{-1/2} \xi_{n+1})^j(g_n^{-1/2} \xi_{n+1})^k \right)^2 \\
&= \sum_{n=0}^{N-1} \mathbb{E}(D^3 u_n(\partial_i, \partial_j, \partial_k)(g_n^{-1/2} \xi_{n+1})^i(g_n^{-1/2} \xi_{n+1})^j(g_n^{-1/2} \xi_{n+1})^k)^2
\end{aligned}
\tag{A.29}$$

Noting that  $\mathbb{E}[D^2 u_n(g_n^{-1/2} \xi_{n+1}, g_n^{-1/2} \xi_{n+1}) - \Delta_M u_n \mid X_n^h] = 0$ , we get

$$\begin{aligned}
& \mathbb{E} \left( \sum_{n=0}^{N-1} D^2 u_n(g_n^{-1/2} \xi_{n+1}, g_n^{-1/2} \xi_{n+1}) - \Delta_M u_n \right)^2 \\
&= \sum_{n=0}^{N-1} \mathbb{E}(D^2 u_n(g_n^{-1/2} \xi_{n+1}, g_n^{-1/2} \xi_{n+1}) - \Delta_M u_n)^2.
\end{aligned}
\tag{A.30}$$

Taking expectation on both sides of (A.26), using (A.27)-(A.30) and applying (2.16), we obtain

$$\mathbb{E}(\tilde{\mu}_{\phi, N}(\varphi) - \mu_{\phi}(\varphi))^2 \leq C \left( h^2 + \frac{1}{T} \right),$$

where  $C > 0$  is a constant independent of  $h$  and  $T$  and it linearly depends on  $\|\varphi\|_{C^{2,\epsilon}(M)}$  but otherwise it is independent of  $\varphi$ .  $\square$

**A.3. Proof of Theorem 3.3.** Consider  $\varphi \in \mathcal{H}$  (see (3.17)). Since  $\mu_\phi^h$  is stationary measure of Markov chain (see Section 3), we have

$$\int_M \varphi(x) \mu_\phi^h(dx) = \int_M \mathbb{E}_x \varphi(X_k^h) \mu_\phi^h(dx),$$

where  $\mathbb{E}_x \varphi(X_k^h)$  implies that Markov chain starts at  $x$ , i.e.  $X_0 = x$ . Therefore, we can write

$$\int_M \varphi(x) \mu_\phi^h(dx) = \int_M \frac{1}{N} \sum_{k=1}^N \mathbb{E}_x \varphi(X_k^h) \mu_\phi^h(dx).$$

Using Theorem 3.2, we get

$$\begin{aligned} \left| \int_M \varphi(x) (\mu_\phi^h(dx) - \mu(dx)) \right| &= \left| \int_M \left( \frac{1}{N} \sum_{k=1}^N \mathbb{E}_x \varphi(X_k^h) - \mu_\phi(\varphi) \right) \mu_\phi^h(dx) \right| \\ &\leq K \left( h + \frac{1}{Nh} \right), \end{aligned}$$

where  $K > 0$  is independent of  $h$ ,  $N$  and  $\varphi$  from  $\mathcal{H}$  (the latter thanks to the constant  $C$  in Theorem 3.2 being dependent on  $\varphi$  only via linear dependence on  $\|\varphi\|_{C^{2,\epsilon}(M)}$  which is bounded for the class  $\mathcal{H}$  of functions  $\varphi$ ). Letting  $N \rightarrow \infty$ , we get the desired result.